Integrative Taxonomy of the Micrura alaskensis Coe, 1901 Species Complex (Nemertea: Heteronemertea), with Descriptions of a New Genus Maculaura gen. nov. and Four New Species from the NE Pacific

Authors: Hiebert, Terra Celeste, and Maslakova, Svetlana

Source: Zoological Science, 32(6) : 615-637

Published By: Zoological Society of Japan

URL: https://doi.org/10.2108/zs150011

ZOOLOGICAL SCIENCE **32**: 615–637 (2015)

Integrative Taxonomy of the *Micrura alaskensis* Coe, 1901 Species Complex (Nemertea: Heteronemertea), with Descriptions of a New Genus *Maculaura* gen. nov. and Four New Species from the NE Pacific

Terra Celeste Hiebert* and Svetlana Maslakova

Oregon Institute of Marine Biology, University of Oregon, Charleston, OR 97420, USA

***Micrura alaskensis* Coe, 1901 is a common intertidal heteronemertean known from eastern and northwest Pacific (Alaska to Ensenada, Mexico and Akkeshi, Japan, respectively). It is an emerging model system in developmental biology research. We present evidence from morphology of the adults, gametes, and sequences of cytochrome c oxidase subunit I and 16S rRNA genes that it is not one, but a complex of five, cryptic species. All five of these species co-occur at least in part of their geographic range (e.g. southern Oregon). Preliminary cross-hybridization experiments suggest that at least some of these species are reproductively isolated. The five species share characteristics of adult morphology (e.g. accessory buccal glands) and at least four are known to possess a unique larval morphotype—*pilidium maculosum.* We propose that these characters define a new genus, *Maculaura* gen. nov., which contains the following five species: *Maculaura alaskensis* comb. nov., *Maculaura aquilonia* sp. nov., *Maculaura cerebrosa* sp. nov., *Maculaura oregonensis* sp. nov., and *Maculaura magna* sp. nov. It is unclear which of the five species Coe originally encountered and described. We chose to retain the name "*alaskensis"* for the species that current researchers know as "*Micrura alaskensis*", although, presently, it is only known from Washington and Oregon, and has not been collected from Alaska. *Maculaura aquilonia* sp. nov. is the only member of the genus we have encountered in Alaska, and we show that it also occurs in the Sea of Okhotsk, Russia.**

Key words: Pilidiophora, Lineidae, Heteronemertea, pilidium, cryptic species

INTRODUCTION

Micrura alaskensis Coe, 1901 is an eyeless pink worm with longitudinal cephalic slits and caudal cirrus. It is one of the most common intertidal nemerteans found in sand flats and under rocks along the Pacific coast of North America, with reported northeastern Pacific occurrence from Alaska to Southern California (Corrêa, 1964; Gibson, 1995; Roe et al., 2007). It was first described by Coe (1901) from several locations in Alaska including Glacier Bay, Sitka, Yakutat, and Prince William Sound. Coe (1905) re-described *Micrura alaskensis* and adjusted the range southward to San Pedro, California. Coe (1940) subsequently synonymized *Micrura griffini* Coe, 1905 with *Micrura alaskensis* and reported *Micrura alaskensis* from Alaska to southern California and Mexico. At the same time, Japanese authors (Yamaoka, 1940; Iwata, 1954) reported the presence of this species in Akkeshi, Japan (Kajihara, 2007). In recent years, *Micrura alaskensis* has become a model for studies of fertilization (e.g. Stricker and Smythe, 2000, 2001, 2003; Stricker et al., 2001, 2013), larval function (Dassow and Maslakova, 2013; Dassow et al., 2013), and development (e.g. Maslakova, 2010; Bird et al., 2014; Swider et al., 2014; Maslakova and Dassow, 2014; Hiebert and Maslakova, 2015) due to its abundance, accessibility, and amenability to embryological work. This species has been used in molecular phylogenies of the phylum (Thollesson and Norenburg, 2003), and its developmental transcriptome has been sequenced and assembled (Meyer et al., in prep.; Hiebert and Maslakova, unpublished). Here, we show that worms that fit the description of *Micura alaskensis* and occur intertidally in southern Oregon possess subtle morphological and not-so-subtle reproductive differences, and form at least five genetically distinct lineages. In other words, *Micrura alaskensis* is clearly not one, but several closely related cryptic species. Furthermore, our preliminary experiments on cross-fertilization between some of these forms support their biological species status. Coe's original description (Coe, 1901) and revisions thereafter (Coe, 1904, 1905, 1940) clearly combine characters (e.g. body color, habitat) from several of these species. Type material does not exist, which makes it impossible to be certain which of the five species served as the basis for the original species description (Coe, 1901). It

* Corresponding author. Tel. : +1-541-888-2581;
Fax : +1-541-888-3250;
E-mail: terrah@uoregon.edu
doi:10.2108/zs150011

seems apparent that subsequent revisions incorporated more than one species (Coe, 1905, 1940). In order to improve nomenclatural stability and preclude species misidentification we re-describe *Micrura alaskensis* and designate a neotype, retaining the original specific name for the lineage that is the subject of many recent studies, and describe the other four as new species, based on new material from Alaska, Washington, Oregon, California, and Russia.

The genus *Micrura,* which currently contains ~12% of all described heteronemertean species (Gibson, 1995), is poorly defined and certainly non-monophyletic (Sundberg and Saur, 1998; Thollesson and Norenburg, 2003; Schwartz, 2009; Andrade et al., 2012; Kvist et al., 2014). As is the case with other nemertean mega-genera, such as *Cerebratulus* and *Lineus,* membership in *Micrura* is based on combinations of non-unique characters of internal anatomy, e.g. proboscis muscle crosses, presence/absence of caudal cirrus, etc. (Schwartz, 2009). The only reasonable solution to this taxonomic problem is to redefine the genus *Micrura* to include only those species that are closely related to the type species, *Micrura fasciolata* Ehrenberg, 1828, and to move all other species to other (new or existing) genera, as appropriate. Although *Micrura alaskensis* fits the rather vague diagnosis of the genus *Micrura* (Ehrenberg, 1828; McIntosh, 1873–1874; Bürger, 1895), it is only distantly related to the type species for this genus in molecular phylogenies (Schwartz, 2009; Hiebert and Maslakova, in prep). Incidentally, uncorrected sequence divergence values between members of the *Micrura alaskensis* species complex and *Micrura fasciolata* are approximately 20% for 16S and 18% for COI sequence data, nearing or exceeding maximum interspecific divergence values for congeneric nemertean species in well-supported monophyletic genera e.g. *Carinoma*, *Riserius*, *Nipponnemertes* (Hiebert and Maslakova, in prep). These five species of the *Micrura alaskensis* complex constitute a monophyletic group based on molecular phylogenies of the Pilidiophora (Hiebert and Maslakova, in prep), and share characters of adult anatomy and larval morphology, supporting the new genus proposed here, *Maculaura* gen. nov.

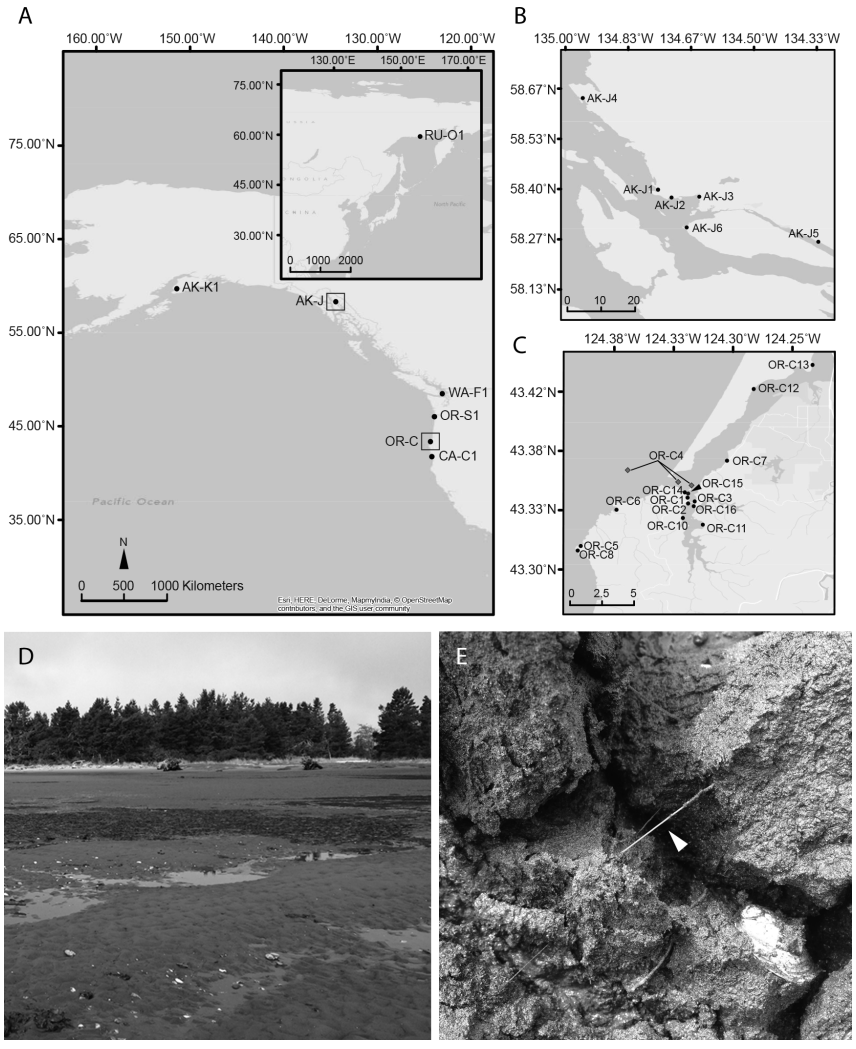

Fig. 1. **(A–C)** Collection sites for members of the "*Micrura alaskensis*" species complex used in this study; **(A)** sampling sites along the shoreline of the northwestern United States in Alaska (AK), Washington (WA), Oregon (OR), and California (CA), and the Sea of Okhotsk in eastern Russia (RU, inset); **(B)** multiple collection sites in Juneau, AK; **(C)** sampling sites in Coos Bay, OR (regions outlined by boxes on A); locations where adult specimens were collected are indicated with closed circles, larval collection sites are shown as diamonds. **(D)** Typical habitat of *Maculaura* spp. is silty sand or mud in protected coves or bays; shown here is North Spit (OR-C13), near Charleston, OR. **(E)** An individual of *Maculaura alaskensis* comb. nov. stretched between mud clods.

MATERIALS AND METHODS

Material examined

Adults

We collected hundreds of adult individuals in the NE Pacific that fit the broad description of *Micrura alaskensis* Coe, 1901 that has emerged over the last hundred years. Collection sites ranged from Juneau, AK to Crescent City, CA (Fig. 1) (collecting-permit numbers: 18512, 18586, 19353, CF-14081). Maps showing geographic locations of all collection sites were generated using ArcGIS ver. 10.2. One adult preserved for molecular analysis was collected in the Sea of Okhotsk near the city of Magadan, Russia and kindly provided by Dr. Alexei V. Chernyshev (Institute of Marine Biology, Far East Branch of the Russian Academy of Sciences). The descriptions herein are based on examination of over 100 specimens (including those used for histology and molecular analysis). See the species descriptions below for detailed information on locations and habitats of each species (Table 1). Type and voucher material is deposited at the National Museum of Natural History, Smithsonian Institution, in Washington, D.C., USA (All NMNH numbers are indicated below using notes) (Table 1). Additional material is kept at the Oregon Institute of Marine Biology, in Charleston, OR, USA (OIMB).

Thirty specimens collected near Juneau, AK were examined

Table 1. Collection information and associated GenBank and USNM numbers. Individual abbreviations correspond to those in Fig. 1 and Fig. 12. Larval specimens are indicated with bold text. The total number of sequences (*n*) used in phylogenetic analyses are shown for each species.

Species	Abbreviation	Collection location	Coordinate	Collector(s)	NMNH Number	Accession Number	
						16S	COI
Maculaura alaskensis	OR-C1-A04	Portside Mudflat, Charleston OR	43.3428°N, 124.3218°W	S. Maslakova		KP682166	–
	OR-C1-C04	Portside Mudflat, Charleston OR	43.3428°N, 124.3218°W	S. Maslakova		KP682167	–
	OR-C1-D04	Portside Mudflat, Charleston OR	43.3428°N, 124.3218°W	S. Maslakova		KP682168	–
	OR-C1-E03	Portside Mudflat, Charleston OR	43.3428°N, 124.3218°W	S. Maslakova		KP682169	–
	OR-C1-E04	Portside Mudflat, Charleston OR	43.3428°N, 124.3218°W	S. Maslakova		KP682170	–
	OR-C1-E5A6	Portside Mudflat, Charleston OR	43.3428°N, 124.3218°W	T. Hiebert		KP682171	–
	OR-C1-E5A7	Portside Mudflat, Charleston OR	43.3428°N, 124.3218°W	T. Hiebert		KP682172	–
	OR-C1-E5A8	Portside Mudflat, Charleston OR	43.3428°N, 124.3218°W	T. Hiebert		KP682173	–
	OR-C1-E5A9	Portside Mudflat, Charleston OR	43.3428°N, 124.3218°W	T. Hiebert		KP682174	–
	OR-C1-F03	Portside Mudflat, Charleston OR	43.3428°N, 124.3218°W	S. Maslakova		KP682175	–
	OR-C1-F04	Portside Mudflat, Charleston OR	43.3428°N, 124.3218°W	S. Maslakova		KP682176	–
	OR-C1-G03	Portside Mudflat, Charleston OR	43.3428°N, 124.3218°W	S. Maslakova		KP682177	–
	OR-C1-M13	Portside Mudflat, Charleston OR	43.3428°N, 124.3218°W	T. Hiebert	1282107	KP682178	KP682051
	OR-C1-M14	Portside Mudflat, Charleston OR	43.3428°N, 124.3218°W	T. Hiebert	1282106 [5]	KP682179	KP682052
	OR-C1-M15	Portside Mudflat, Charleston OR	43.3428°N, 124.3218°W	T. Hiebert	1282108	KP682180	KP682053
	OR-C1-M16	Portside Mudflat, Charleston OR	43.3428°N, 124.3218°W	T. Hiebert	1282109	KP682181	KP682054
	OR-C1-M17	Portside Mudflat, Charleston OR	43.3428°N, 124.3218°W	T. Hiebert		KP682182	KP682055 [3]
	OR-C1-M18	Portside Mudflat, Charleston OR	43.3428°N, 124.3218°W	T. Hiebert		KP682183	KP682056
	OR-C1-M19	Portside Mudflat, Charleston OR	43.3428°N, 124.3218°W	T. Hiebert		KP682184	KP682057
	OR-C1-MMB8	Portside Mudflat, Charleston OR	43.3428°N, 124.3218°W	T. Hiebert		–	KP682058
	OR-C1-MMB9	Portside Mudflat, Charleston OR	43.3428°N, 124.3218°W	T. Hiebert		–	KP682059
	OR-C10-M29	Collver Cove, Charleston OR	43.3272°N, 124.3263°W	T. Hiebert	1282110	–	KP682062
	OR-C10-M30	Collver Cove, Charleston OR	43.3272°N, 124.3263°W	T. Hiebert	1282111	–	KP682063
	OR-C10-M31	Collver Cove, Charleston OR	43.3272°N, 124.3263°W	T. Hiebert		KP682189	KP682064
	OR-C10-M33	Collver Cove, Charleston OR	43.3272°N, 124.3263°W	T. Hiebert		KP682190	KP682065
	OR-C10-M34	Collver Cove, Charleston OR	43.3272°N, 124.3263°W	T. Hiebert		KP682191	KP682066
	OR-C10-M35	Collver Cove, Charleston OR	43.3272°N, 124.3263°W	T. Hiebert		KP682192	KP682067
	OR-C12-M23	North Spit Boat Ramp, North Bend OR	43.4168°N, 124.2755°W	T. Hiebert		KP682193	KP682068
	OR-C12-M22	North Spit Boat Ramp, North Bend OR	43.4168°N, 124.2755°W	T. Hiebert		KP682194	–
	OR-C12-M24	North Spit Boat Ramp, North Bend OR	43.4168°N, 124.2755°W	T. Hiebert		KP682195	KP682069
	OR-C15-M5	Outer Boat Basin, Charleston OR	43.3445°N, 124.3215°W	T. Hiebert		KP682196	KP682070
	OR-C2-103	High Tide Mudflat, Charleston OR	43.3379°N, 124.3247°W	T. Hiebert & S. Maslakova		–	KP682060
	OR-C2-104	High Tide Mudflat, Charleston OR	43.3379°N, 124.3247°W	T. Hiebert & S. Maslakova		KP682185	KP682061
	OR-C4-E4G8	**Outer Boat Basin, Charleston OR**	**43.3445°N, 124.3215°W**	**T. Hiebert**		**KP682186**	**–**
	OR-C7-66	Domehouse Mudflat, Charleston OR	43.3691°N, 124.2981°W	S. Maslakova		KP682187	–
	OR-C8-E2H6	Middle Cove Cape Arago, Charleston OR	43.3033°N, 124.4017°W	T. Hiebert & S. Maslakova		KP682188	–
	OR-S1-E3B7	Necanicum River, Gearhart OR	46.0159°N, 123.9202°W	T. Hiebert		KP682197	KP682071
	OR-S1-E3B8	Necanicum River, Gearhart OR	46.0159°N, 123.9202°W	T. Hiebert		KP682198	KP682072
	OR-S1-E3B9	Necanicum River, Gearhart OR	46.0159°N, 123.9202°W	T. Hiebert		KP682199	KP682073
	WA-F1-M11	False Bay, San Juan Island WA	48.4855°N, 123.0699°W	S. Maslakova		KP682200	KP682075
	WA-F1-M12	False Bay, San Juan Island WA	48.4855°N, 123.0699°W	S. Maslakova		KP682201	KP682076
	WA-F1-M13	False Bay, San Juan Island WA	48.4855°N, 123.0699°W	S. Maslakova		KP682202	KP682077
	WA-F1-M14	False Bay, San Juan Island WA	48.4855°N, 123.0699°W	S. Maslakova		KP682203	KP682078
	WA-F1-M15	False Bay, San Juan Island WA	48.4855°N, 123.0699°W	S. Maslakova		KP682204	KP682079
	WA-F1-M16	False Bay, San Juan Island WA	48.4855°N, 123.0699°W	S. Maslakova		–	KP682080
	WA-F1-M18	False Bay, San Juan Island WA	48.4855°N, 123.0699°W	S. Maslakova		KP682205	KP682081
	WA-F1-M19	False Bay, San Juan Island WA	48.4855°N, 123.0699°W	S. Maslakova		KP682206	KP682082
	WA-F1-M20	False Bay, San Juan Island WA	48.4855°N, 123.0699°W	S. Maslakova		KP682207	KP682074
						n = 42	n = 32
Maculaura aquilonia	AK-J1-E4B7	Lena Beach, Juneau AK	58.3952°N, 134.7512°W	L. Hiebert		KP682208	KP682084
	AK-J1-E4B8	Lena Beach, Juneau AK	58.3952°N, 134.7512°W	L. Hiebert		–	KP682085
	AK-J1-E4B9	Lena Beach, Juneau AK	58.3952°N, 134.7512°W	L. Hiebert		KP682209	KP682086
	AK-J1-E4C1	Lena Beach, Juneau AK	58.3952°N, 134.7512°W	L. Hiebert		KP682210	KP682087
	AK-J1-E4C2	Lena Beach, Juneau AK	58.3952°N, 134.7512°W	L. Hiebert		KP682211	KP682088
	AK-J1-J1	Lena Beach, Juneau AK	58.3952°N, 134.7512°W	T. Hiebert	1282113 [2]	KP682212	–
	AK-J1-J5	Lena Beach, Juneau AK	58.3952°N, 134.7512°W	T. Hiebert		KP682213	KP682089
	AK-J2-J10	Auke Bay, Juneau AK	58.3777°N, 134.7239°W	T. Hiebert		KP682214	KP682090
	AK-J2-J11	Auke Bay, Juneau AK	58.3777°N, 134.7239°W	T. Hiebert		KP682215	KP682091
	AK-J2-J12	Auke Bay, Juneau AK	58.3777°N, 134.7239°W	T. Hiebert		KP682216	KP682092
	AK-J3-J15	Auke Creek, Juneau AK	58.3806°N, 134.6433°W	T. Hiebert		KP682217	KP682093
	AK-J3-J16	Auke Creek, Juneau AK	58.3806°N, 134.6433°W	T. Hiebert		KP682218	KP682094

Continued.

Table 1. Continued.

Species	Abbreviation	Collection location	Coordinate	Collector(s)	NMNH Number	Accession Number	
						16S	COI
	AK-J3-J17	Auke Creek, Juneau AK	58.3806°N, 134.6433°W	T. Hiebert		KP682219	–
	AK-J3-J18	Auke Creek, Juneau AK	58.3806°N, 134.6433°W	T. Hiebert		KP682220	KP682095
	AK-J3-J19	Auke Creek, Juneau AK	58.3806°N, 134.6433°W	T. Hiebert		KP682221	KP682096
	AK-J3-J20	Auke Creek, Juneau AK	58.3806°N, 134.6433°W	T. Hiebert		KP682222	KP682097
	AK-J3-J22	Auke Creek, Juneau AK	58.3806°N, 134.6433°W	T. Hiebert		KP682223	KP682098
	AK-J3-J23	Auke Creek, Juneau AK	58.3806°N, 134.6433°W	T. Hiebert		KP682224	KP682099
	AK-J4-J36	Bridget Cove, Juneau AK	58.6358°N, 134.9462°W	T. Hiebert		KP682225	KP682100
	AK-J5-J45	Sheep Creek, Juneau AK	58.2608°N, 134.3256°W	T. Hiebert		KP682226	KP682101
	AK-J5-J46	Sheep Creek, Juneau AK	58.2608°N, 134.3256°W	T. Hiebert		KP682227	KP682102
	AK-J6-J48	Outer Point Douglas, Juneau AK	58.3004°N, 134.6779°W	T. Hiebert		KP682228	KP682103
	AK-J6-J49	Outer Point Douglas, Juneau AK	58.3004°N, 134.6779°W	T. Hiebert		KP682229	KP682104
	AK-J6-J50	Outer Point Douglas, Juneau AK	58.3004°N, 134.6779°W	T. Hiebert		KP682230	KP682105
	AK-J6-J51	Outer Point Douglas, Juneau AK	58.3004°N, 134.6779°W	T. Hiebert		KP682231	KP682106
	AK-J6-J52	Outer Point Douglas, Juneau AK	58.3004°N, 134.6779°W	T. Hiebert		KP682232	KP682107
	AK-J6-J53	Outer Point Douglas, Juneau AK	58.3004°N, 134.6779°W	T. Hiebert		KP682233	KP682108
	AK-J6-J54	Outer Point Douglas, Juneau AK	58.3004°N, 134.6779°W	T. Hiebert		KP682234	KP682109
	AK-J6-J55	Outer Point Douglas, Juneau AK	58.3004°N, 134.6779°W	T. Hiebert	1282114 [2]	KP682235	KP682110
	AK-J6-J56	Outer Point Douglas, Juneau AK	58.3004°N, 134.6779°W	T. Hiebert	1282115 [2]	KP682236	KP682111
	AK-J6-J57	Outer Point Douglas, Juneau AK	58.3004°N, 134.6779°W	T. Hiebert		KP682237	KP682112
	AK-J6-J58	Outer Point Douglas, Juneau AK	58.3004°N, 134.6779°W	T. Hiebert		KP682238	KP682113
	AK-J6-J59	Outer Point Douglas, Juneau AK	58.3004°N, 134.6779°W	T. Hiebert		KP682239	KP682114
	AK-J6-J60	Outer Point Douglas, Juneau AK	58.3004°N, 134.6779°W	T. Hiebert	1282116 [2]	KP682240	KP682115
	OR-C10-E2G2	Collver Cove, Charleston OR	43.3272°N, 124.3263°W	T. Hiebert & S. Maslakova		KP682244	KP682126
	OR-C10-E2G3	Collver Cove, Charleston OR	43.3272°N, 124.3263°W	T. Hiebert & S. Maslakova		KP682245	KP682127
	OR-C10-E3A3	Collver Cove, Charleston OR	43.3272°N, 124.3263°W	T. Hiebert & S. Maslakova		KP682246	KP682128
	OR-C10-M32	Collver Cove, Charleston OR	43.3272°N, 124.3263°W	T. Hiebert	1282117 [2]	KP682247	KP682129
	OR-C10-M37	Collver Cove, Charleston OR	43.3272°N, 124.3263°W	T. Hiebert	1282118	KP682248	KP682130 [3]
	OR-C12-M20	North Spit Boat Ramp, North Bend OR	43.4168°N, 124.2755°W	T. Hiebert		KP682249	KP682131
	OR-C2-102	High Tide Mudflat, Charleston OR	43.3379°N, 124.3247°W	T. Hiebert & S. Maslakova		KP682241	KP682122
	OR-C4-205	**Outer Boat Basin, Charleston OR**	**43.3445°N, 124.3215°W**	**G. von Dassow**		**KP682243**	**–**
	OR-C4-82	**Outer Boat Basin, Charleston OR**	**43.3445°N, 124.3215°W**	**S. Maslakova**		**KP682242**	**KP682124**
	RU-O1	Sea of Okhotsk, Magadan RUSSIA	59.5620°N, 150.7444°W	A. Chernyshev		KP682250	KP682133
	AK-K1-A2	Kachemak Bay, AK	59.4677°N, 151.5565°W	S. Maslakova & J. Norenburg		–	KP682116
	AK-K1-C1	Kachemak Bay, AK	59.4677°N, 151.5565°W	S. Maslakova & J. Norenburg		–	KP682117
	AK-K1-C2	Kachemak Bay, AK	59.4677°N, 151.5565°W	S. Maslakova & J. Norenburg		–	KP682118
	AK-K1-D1	Kachemak Bay, AK	59.4677°N, 151.5565°W	S. Maslakova & J. Norenburg		–	KP682119
	AK-K1-E1	Kachemak Bay, AK	59.4677°N, 151.5565°W	S. Maslakova & J. Norenburg		–	KP682120
	AK-K1-F4	Kachemak Bay, AK	59.4677°N, 151.5565°W	S. Maslakova & J. Norenburg		–	KP682121
	AK-K1-G1	Kachemak Bay, AK	59.4677°N, 151.5565°W	S. Maslakova & J. Norenburg		–	KP682083
	OR-C16-M2	Qualman Mudlfat, Charleston OR	43.3382°N, 124.3206°W	T. Hiebert	1282112 [1]	–	KP682132
	OR-C4-213	**Outer Boat Basin, Charleston OR**	**43.3445°N, 124.3215°W**	**G. von Dassow**		**–**	**KP682125**
	OR-C4-81	**Outer Boat Basin, Charleston OR**	**43.3445°N, 124.3215°W**	**L. Hiebert**		**–**	**KP682123**
						n = 43	n = 51
Maculaura cerebrosa	CA-C1-E1A8	Crescent City, CA	41.7362°N, 124.1744°W	G. Paulay		KP682251	KP682134
	OR-C10-M36	Collver Cove, Charleston OR	43.3272°N, 124.3263°W	T. Hiebert		KP682259	KP682138
	OR-C13-M11	North Spit, North Bend OR	43.4366°N, 124.2338°W	T. Hiebert	1282120 [2]	KP682260	KP682139
	OR-C13-M12	North Spit, North Bend OR	43.4366°N, 124.2338°W	T. Hiebert	1282121 [2]	KP682261	KP682140
	OR-C14-M10	Inner Boat Basin, Charleston OR	43.3465°N, 124.3272°W	T. Hiebert		KP682263	KP682142
	OR-C14-M9	Inner Boat Basin, Charleston OR	43.3465°N, 124.3272°W	T. Hiebert		KP682262	KP682141
	OR-C15-M3	Outer Boat Basin, Charleston OR	43.3445°N, 124.3215°W	T. Hiebert	1282119 [1]	KP682264	KP682143
	OR-C15-M4	Outer Boat Basin, Charleston OR	43.3445°N, 124.3215°W	T. Hiebert		KP682265	KP682144
	OR-C15-M6	Outer Boat Basin, Charleston OR	43.3445°N, 124.3215°W	T. Hiebert	1282122 [2]	KP682266	KP682145
	OR-C15-M7	Outer Boat Basin, Charleston OR	43.3445°N, 124.3215°W	T. Hiebert	1282124	KP682267	KP682146 [3]
	OR-C2-107	High Tide Mudflat, Charleston OR	43.3379°N, 124.3247°W	T. Hiebert & S. Maslakova	1282123 [2]	KP682252	–
	OR-C4-196	**Outer Boat Basin, Charleston OR**	**43.3445°N, 124.3215°W**	**T. Hiebert**		**KP682253**	**–**
	OR-C6-2008	Outer Boat Basin, Charleston OR	43.3445°N, 124.3215°W	S. Maslakova		KP682256	–
	OR-C4-210	**Outer Boat Basin, Charleston OR**	**43.3445°N, 124.3215°W**	**T. Hiebert**		**KP682254**	**–**
	OR-C4-211	**Outer Boat Basin, Charleston OR**	**43.3445°N, 124.3215°W**	**T. Hiebert**		**KP682255**	**KP682135**
	OR-C5-173	North Cove Cape Arago, Charleston OR	43.3096°N, 124.3991°W	S. Maslakova		KP682257	KP682136
	OR-C6-30	Sunset Bay, Charleston OR	43.3347°N, 124.3756°W	S. Maslakova		KP682258	KP682137
						n = 17	n = 13
Maculaura magna	OR-C1-M8	Portside Mudflat, Charleston OR	43.3428°N, 124.3218°W	T. Hiebert	1282125 [1]	KP682268	KP682147 [4]
	OR-C2-105	High Tide Mudflat, Charleston OR	43.3379°N, 124.3247°W	T. Hiebert & S. Maslakova		KP682270	KP682148
	OR-C2-13	High Tide Mudflat, Charleston OR	43.3379°N, 124.3247°W	S. Maslakova		KP682269	–

Continued.

Table 1. Continued.

Species	Abbreviation	Collection location	Coordinate	Collector(s)	NMNH Number	Accession Number	
						16S	COI
	OR-C3-93	Fisherman's Grotto Mudflat, Charleston OR	43.3419°N, 124.3193°W	T. Hiebert & S. Maslakova		KP682271	KP682150
	OR-C3-95	Fisherman's Grotto Mudflat, Charleston OR	43.3419°N, 124.3193°W	T. Hiebert & S. Maslakova		KP682272	–
	OR-C3-96	Fisherman's Grotto Mudflat, Charleston OR	43.3419°N, 124.3193°W	T. Hiebert & S. Maslakova		KP682273	KP682151
	OR-C4-112	**Outer Boat Basin, Charleston OR**	**43.3445°N, 124.3215°W**	**T. Hiebert**		**KP682274**	**KP682152**
	OR-C4-131	**Outer Boat Basin, Charleston OR**	**43.3445°N, 124.3215°W**	**T. Hiebert**		**KP682275**	**–**
	OR-C4-177	**Outer Boat Basin, Charleston OR**	**43.3445°N, 124.3215°W**	**T. Hiebert**		**KP682276**	**–**
	OR-C4-E3A6	**Outer Boat Basin, Charleston OR**	**43.3445°N, 124.3215°W**	**T. Hiebert**		**KP682277**	**–**
	OR-C4-E3H4	**Outer Boat Basin, Charleston OR**	**43.3445°N, 124.3215°W**	**T. Hiebert**		**KP682278**	**–**
	OR-C4-E3H6	**Outer Boat Basin, Charleston OR**	**43.3445°N, 124.3215°W**	**T. Hiebert**		**KP682279**	**–**
	OR-C4-E3I1	**Outer Boat Basin, Charleston OR**	**43.3445°N, 124.3215°W**	**T. Hiebert**		**KP682280**	**–**
	OR-C4-E3I3	**Outer Boat Basin, Charleston OR**	**43.3445°N, 124.3215°W**	**T. Hiebert**		**KP682281**	**–**
	OR-C4-E3I5	**Outer Boat Basin, Charleston OR**	**43.3445°N, 124.3215°W**	**T. Hiebert**		**KP682282**	**KP682153**
	OR-C4-LWB7	**Outer Boat Basin, Charleston OR**	**43.3445°N, 124.3215°W**	**T. Hiebert**		**KP682283**	**–**
	OR-C4-LWB8	**Outer Boat Basin, Charleston OR**	**43.3445°N, 124.3215°W**	**T. Hiebert**		**KP682284**	**–**
	OR-C4-LWB9	**Outer Boat Basin, Charleston OR**	**43.3445°N, 124.3215°W**	**T. Hiebert**		**KP682285**	**–**
	OR-C4-LWC1	**Outer Boat Basin, Charleston OR**	**43.3445°N, 124.3215°W**	**T. Hiebert**		**KP682286**	**–**
	OR-C4-LWC2	**Outer Boat Basin, Charleston OR**	**43.3445°N, 124.3215°W**	**T. Hiebert**		**KP682287**	**–**
	OR-C4-LWC7	**Outer Boat Basin, Charleston OR**	**43.3445°N, 124.3215°W**	**T. Hiebert**		**KP682288**	**–**
	OR-C4-LWC8	**Outer Boat Basin, Charleston OR**	**43.3445°N, 124.3215°W**	**T. Hiebert**		**KP682289**	**–**
	OR-C4-LWD7	**Outer Boat Basin, Charleston OR**	**43.3445°N, 124.3215°W**	**T. Hiebert**		**KP682290**	**–**
	OR-C4-LWE6	**Outer Boat Basin, Charleston OR**	**43.3445°N, 124.3215°W**	**T. Hiebert**		**KP682291**	**–**
	OR-C5-162	North Cove Cape Arago, Charleston OR	43.3096°N, 124.3991°W	S. Maslakova		KP682292	–
	OR-C5-163	North Cove Cape Arago, Charleston OR	43.3096°N, 124.3991°W	S. Maslakova		KP682293	KP682154
	OR-C6-174	Sunset Bay, Charleston OR	43.3347°N, 124.3756°W	S. Maslakova		KP682294	KP682155
	OR-C6-175	Sunset Bay, Charleston OR	43.3347°N, 124.3756°W	S. Maslakova		KP682295	KP682156
	OR-C2-159	High Tide Mudflat, Charleston OR	43.3379°N, 124.3247°W	T. Hiebert & S. Maslakova		–	KP682149
	OR-C3-M42	Fisherman's Grotto Mudflat, Charleston OR	43.3419°N, 124.3193°W	T. Hiebert	1282126 [2]	–	–
	OR-C1-M43	Portside Mudflat, Charleston OR	43.3428°N, 124.3218°W	T. Hiebert & S. Maslakova	1282127 [2]	–	–
						n = 28	n = 10
Maculaura oregonensis	OR-C10-M25	Collver Cove, Charleston OR	43.3272°N, 124.3263°W	T. Hiebert	1282128 [1]	KP682299	KP682159 [4]
	OR-C10-M26	Collver Cove, Charleston OR	43.3272°N, 124.3263°W	T. Hiebert	1282129 [2]	KP682300	KP682160
	OR-C11-E2I6	Brown's Cove, Charleston OR	43.3234°N, 124.3144°W	T. Hiebert & S. Maslakova		KP682301	KP682163
	OR-C13-E5B3	North Spit, North Bend OR	43.4366°N, 124.2338°W	T. Hiebert		KP682302	–
	OR-C13-MMB12	North Spit, North Bend OR	43.4366°N, 124.2338°W	T. Hiebert		KP682303	–
	OR-C13-MMB13	North Spit, North Bend OR	43.4366°N, 124.2338°W	T. Hiebert		KP682304	KP682164
	OR-C3-94	Fisherman's Grotto Mudflat, Charleston OR	43.3419°N, 124.3193°W	T. Hiebert & S. Maslakova		KP682298	–
	OR-C10-M27	Collver Cove, Charleston OR	43.3272°N, 124.3263°W	T. Hiebert		–	KP682161
	OR-C10-M28	Collver Cove, Charleston OR	43.3272°N, 124.3263°W	T. Hiebert		–	KP682162
	OR-C1-E4A2	Portside Mudflat, Charleston OR	43.3428°N, 124.3218°W	T. Hiebert		KP682297	KP682158
	OR-C1-E3G6	Portside Mudflat, Charleston OR	43.3428°N, 124.3218°W	T. Hiebert		KP682296	KP682157
						n = 9	n = 8

[1]holotype, [2]paratype, [3]topogenetype, [4]hologenetype, [5]neotype

externally and preserved for molecular analysis at the University of Alaska, Southeast (UAS). All other specimens were examined at the OIMB. Live worms were kept in 150-ml glass dishes submerged in a sea table with running seawater at ambient sea temperature. Adults were photographed using a Leica DFC400 digital camera mounted to a Leica MZ10F dissecting microscope and accompanying software (Leica Application Suite ver. 3.6) at OIMB.

Larvae

Twenty-six pilidium larvae were collected using a plankton net (SeaGear, 0.5-m diameter with 153-μm mesh) in Coos Bay, from the Charleston marina docks or by boat in the Charleston Channel (OR-C4, Fig. 1C). Larvae were photographed individually using the same camera and software as above and an Olympus BX51 compound microscope equipped with differential interference contrast optics. For photography, larvae were gently trapped between glass slide and cover slip supported by small clay feet. Young wild-caught larvae were reared in the lab on a diet of the unicellular cryptophyte alga *Rhodomonas lens* (Pascher and Ruttner, CCMP739) in bowls of filtered seawater (FSW, 0.45 μm) for up to 10 weeks and periodically photographed. Larval identity was confirmed using DNA sequence data as described below.

Embryonic cultures

To characterize development, embryonic cultures were established in the lab when gravid males and females of each species were available, and larvae were reared to metamorphosis as previously described by Maslakova (2010). To further confirm the species status of the five lineages, we carried out cross-fertilization experiments between different forms when reproductive adults of more than one form were available. Cross-fertilization was initially attempted with the same sperm concentrations (~1/1000) for embryonic culturing of con-specifics but was increased over time to ensure that sperm concentration was not a limiting factor and to promote hybridization.

Molecular analysis

Tissue from 128 adults was preserved for molecular analysis. Two small (2 × 2 mm) pieces of tissue were preserved from each individual (one cryopreserved and kept at –80°C, and the other immersed in 80% EtOH and kept at –20°C). DNA extraction from adult tissue was carried out using a DNeasy Blood and Tissue Kit

(Qiagen) or Wizard SV Genomic DNA Purification System (Promega). Tissue lysis was performed in a Nuclei Lysis solution composed of 0.5 M EDTA and proteinase K (20 mg/ml) at 56°C for 6–12 h. Twenty-six larvae were cryopreserved whole in a small volume (< 10 μl) of FSW at –80°C after being photographed. PCR-quality DNA was obtained from larvae using Chelex matrix (InstaGene, BioRad) with initial incubation at 56°C for 30 min followed by a short (8 min) incubation at 98°C.

"Barcoding" regions of two mitochondrial genes were amplified: 16S rRNA (460–537 bp, 16S) and cytochrome *c* oxidase subunit I (658–698 bp, COI). PCR amplification was carried out with universal primers: 16SARL [5′ CGCCTGTTTATCAAAAACAT 3′] and 16S BRH [5′ CCGGTCTGAACTCAGATCACGT 3′] (Palumbi et al., 1991); LCO 1490 [5′ GGTCAACAAATCATAAAGATATTGG 3′] and HCO 2198 [5′ TAAACTTCAGGGTGACCAAAAAATCA 3′] (Folmer et al., 1994). Occasionally, higher quality amplification was achieved by pairing nemertean-specific reverse primers (16SKR [5′ AATAGATAGAAACCAACCTGGC 3′], COIDr [5′ GAGAAATAATACCAAAACCAGG 3′] (Norenburg, unpublished)) with corresponding universal forward primers. PCR thermocycling was carried out using 1–8 μl of DNA extract in a 20-μl reaction volume with the following parameters: 95°C initial denaturation for 2 min, 35 cycles of 95°C for 40 s, 45–55°C for 40 s and a 60-s extension at 72°C. Following the last cycle there was an additional 2 min at 72°C for final extension after which products were stored at 4°C. PCR products were purified using Wizard SV Gel and PCR Cleanup kit (Promega) and sequenced (Sequetech Inc, Mountain View, CA) in both directions using forward and reverse primers to maximize sequence length and accuracy. COI sequence data from specimens collected near the Kasitsna Bay Laboratory (NOAA) in Kachemak Bay, AK (AK-K1, Fig. 1A) were provided by Dr. Jon L. Norenburg (Smithsonian Institution). Sequences were trimmed to remove primers, assembled in contigs, proofread for quality using Geneious ver. 7.0.6, and deposited in GenBank (accession numbers KP682050–KP682304).

Histology

Adults were relaxed in a 1:1 mixture of $MgCl_2$ and FSW for 30–60 min and preserved for histology in 10% buffered formalin for at least 24 h, then post-fixed in Hollande-Bouin's Fixative (Electron Microscopy Sciences, Hatfield, PA) for 24–72 h, rinsed in 70% EtOH until all traces of Bouin's were removed, as assessed by the color of solution (solution exchanged at least once daily for 10 days) and stored in 70% EtOH until processed. Specimens were dehydrated through an EtOH series, cleared with several washes in xylene and embedded in paraffin (56°C, melting point). Slides with serial sections of 7–8 μm thickness were stained with Crandall's polychrome method—a combination of the Mallory, Gomori, Koneff and Gurr-McConail techniques where time in red stain and counter stain were slightly modified to 3 and 4 min, respectively—and mounted using Permount (Electron Microscopy Sciences, Hatfield, PA). Sections were imaged using an Olympus BX51 compound microscope, Leica DFC400 digital camera and Leica Application Suite ver. 3.6 software.

Alignment, phylogenetic analysis, haplotype networks, and species delimitation

Our phylogenetic, statistical parsimony, and species delimitation analyses were performed on 139 (16S) and 114 (COI) sequences, which were trimmed to the same length to minimize missing data (440 bp for 16S and 512 for COI). Sequences were aligned using ClustalW (gap opening and extension costs set to default parameters, 15 and 6.66, respectively) as implemented in Geneious ver. 7.0.6 (Biomatters Ltd). Sequence divergence values were calculated as uncorrected *p*-distances (and converted to percentage) from pairwise sequence alignments in Geneious ver. 7.0.6. Maximum likelihood phylogenetic analysis was carried out including 139 (16S) and 114 (COI) sequences using PhyML ver. 3.0 (Guindon et al., 2010) with TN93 (Tamura and Nei, 1993) substitution model and default parameters. Clade support was estimated using 1000 bootstrap replicates (Felsenstein, 1985). Bayesian phylogenetic analyses were conducted in MrBayes ver. 3.2.1 (Ronquist et al., 2012) where evolutionary model parameters for each gene region were TN93 (Tamura and Nei, 1993) selected by jModel-Test ver. 2.1 (Posada, 2008) as the best-fit model. Four chains were run for 1,000,000 generations, sampling trees every 1000 generations, excluding the first 25% discarded as burn-in. Gene tree topologies were viewed in FigTree ver. 1.3.1 (Rambaut, 2009) or Geneious ver. 7.0.6. Sequences from another member of the family Lineidae, *Lineus flavescens* Coe, 1904, were used as an outgroup to root the trees. This individual (*L. flavescens*) was collected from along the South Slough estuary in Charleston, OR (OR-C10, Fig. 1C, GenBank accession numbers KP682165 (16S) and KP682050 (COI)). Haplotype networks were generated with TCS ver. 1.21 (Clement et al., 2000) based on 95% confidence intervals using 136 (16S) and 115 (COI) sequences. Two additional DNA taxonomy methods were used on the same 16S and COI sequences, including a Bayesian implementation of the Poisson Tree Processes model (bPTP, Zhang et al., 2013) and the Automatic Barcode Gap Discovery (ABGD, Puillandre et al., 2012) method. ABGD analysis was carried out using default parameters (P-min 0.001, P-max 0.1, steps 10, gap width 1.5). Default parameters were also used for bPTP (thinning 100, burn-in 0.1, seed 123), which was run on a maximum likelihood tree (PhyML), with 500,000 MCMC generations 500,000 with convergence checked for each analysis (Zhang et al., 2013; Leasi and Norenburg, 2014).

RESULTS

Taxonomy

PILIDIOPHORA Thollesson and Norenburg, 2003
Class **HETERONEMERTEA**
Family **LINEIDAE** McIntosh, 1874

Genus ***Maculaura*** gen. nov.

Type species. *Micrura alaskensis* Coe, 1901, fixed by original designation.

Etymology. The generic name is feminine in gender, neologized by combining the first part of the Latin *maculosus* (having spots, spotted) and *aura* (air, breeze) in reference to the characteristic spotted pigmentation of the thin veil-like amnion surrounding the juvenile inside the pilidium larva, a suspected synapomorphy of this genus (*pilidium maculosum* morphotype, Fig. 2A).

Diagnosis. Body wall of typical heteronemertean composition with outer and inner longitudinal muscle layers separated by middle circular layer; middle circular muscle layer thickens in posterior esophageal region; outer dermis markedly glandular; sub-epithelial foregut glands—referred to as "accessory buccal glands" by Coe (1901)—associated with buccal cavity and extending into ventral outer longitudinal musculature; proboscis unbranched and unarmed, with four muscle layers including outer and inner (endothelial) circular, longitudinal and, sometimes inconspicuous, diagonal muscle layer—i.e., the musculature is "modified heterotype" according to Chernyshev (2015); two proboscis muscle crosses present, although sometimes thin; outer longitudinal musculature in proboscis absent or present as two muscle strands outside main proboscis nerves; rhynchocoel with outer circular and inner longitudinal muscle layers, not consistently interwoven with body wall musculature; dorsal

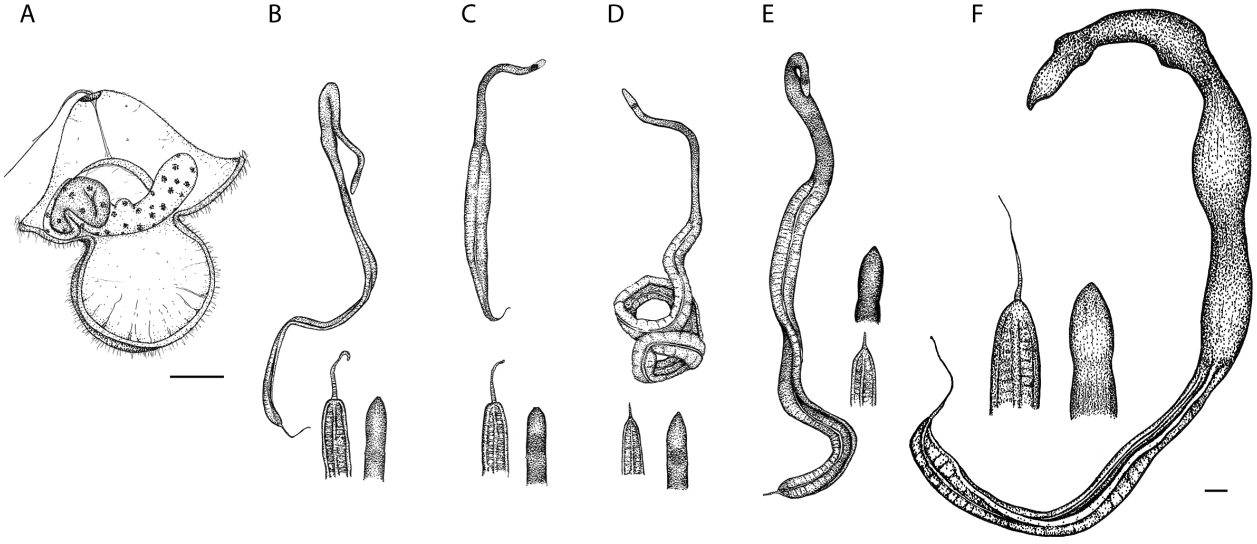

Fig. 2. Comparison of five species in *Maculaura* gen. nov. **(A)** The *pilidium maculosum* larval morphotype. **(B–F)** External appearance of adults: **(B)** *Maculaura alaskensis* (Coe, 1901) comb. nov., **(C)** *Maculaura aquilonia* sp. nov., **(D)** *Maculaura cerebrosa* sp. nov., **(E)** *Maculaura oregonensis* sp. nov., **(F)** *Maculaura magna* sp. nov. Scale bars: 100 μm (A) and 1 mm (B–F).

ganglia separate posteriorly into upper and lower neuropil; neurochord cells absent; inner and outer neurilemma present; external color of live worms pale to dark pink, sometimes white anteriorly; lateral cephalic slits relatively shallow compared to those in other lineids (A. V. Chernyshev, pers. comm.); ocelli lacking at all stages of development as well as in adults; head shape ovate to rectangular, with obtuse apex (Fig. 2B–F), not distinctly marked from the rest of body (i.e. posterior margins of lateral slits linear), except when contracted; body oval in cross-section in foregut region, dorso-ventrally flattened in midgut region; lateral body margins not sharp; worms glide, but do not swim; caudal cirrus present and regenerated easily if lost; gonochoric, with gonads serially arranged and alternating with intestinal diverticula; fertilization occurs externally in water column (i.e. broadcast spawning); oocytes 75–125 μm, with or without chorion; sperm morphology modified or primitive with headpiece size 5–15 μm long (Fig. 3); with planktotrophic pilidium larva of "*gyrans*" type with conspicuous reddish, black, or brown pigment spots decorating the juvenile amnion (*pilidium maculosum*).

Composition. This genus includes five species: *Maculaura alaskensis* comb. nov., *Maculaura aquilonia* sp. nov., *Maculaura cerebrosa* sp. nov., *Maculaura magna* sp. nov., and *Maculaura oregonensis* sp. nov. (Fig. 2B–F).

Geographic distribution. The geographic distribution of this genus, as confirmed by DNA sequence data, includes the NE Pacific: Alaska (Juneau and Kachemak Bay), Washington (False Bay, San Juan Island), Oregon (Seaside, Coos Bay, Charleston), and California (Crescent City); and the NW Pacific (the Sea of Okhotsk, Russia) (Fig. 1A). Additional records, awaiting confirmation by DNA sequence data, include various locations in Alaska: Glacier Bay, Sitka, Yakutat, Prince William Sound (Coe, 1901), British Columbia (Coe, 1940), southern California to Ensenada, Mexico (Coe, 1940), and Hokkaido, Japan (Yamaoka, 1940; Iwata, 1954; Gibson, 1995; Roe et al., 2007; Kajihara, 2007). Numerous larvae that were confirmed to belong to this genus have been collected from Coos Bay, OR. Larvae of this morphotype have also been found in plankton near Bamfield, B.C., Canada (Lacalli, 2005).

Maculaura alaskensis (Coe, 1901) comb. nov.
(Figs. 2B, 3A–B, 4A–B, 5, 6)

Micrura alaskensis Coe, 1901, in part.

Etymology. The specific epithet is an adjective (*-ensis*, *-ense*), referring to the geographic origin of specimens originally described by Coe (1901).

Type material. Morphological types do not exist. We hereby designate a series of transverse histological sections (18 slides # 1282106) and associated ethanol-preserved material from an individual collected from a mudflat in Charleston, OR by T. Hiebert (Table 1) as the neotype, according to Article 75.3 of the Code (ICZN, 1999). Neotype is deposited at the NMNH. We further designate a partial COI sequence from a different individual collected from the same location as a topogenetype (GenBank accession number KP682055, Table 1).

Material examined. Forty-seven adult individuals (collected from False Bay, San Juan Island, WA as well as locations in or near Gearhart and Charleston, OR) and one wild-caught larva were examined and their identification confirmed by DNA sequence data (see Table 1 for GenBank accession numbers). These included serial transverse histological sections of two individuals (36 slides # 1282107 and 18 slides, neotype, # 1282106), and four whole specimens preserved for histology (#s 1282108–1282111); ethanol-preserved tissue from all six specimens is deposited at the NMNH (Table 1). Ethanol-preserved tissue and/or extracted DNA from remaining individuals are held at the OIMB.

Diagnosis. *Maculaura alaskensis* comb. nov. differs from *M. magna* sp. nov. and *M. oregonensis* sp. nov. by its smaller size, narrower body, and not as pink body color. It most closely resembles *M. aquilonia* sp. nov. and *M. cerebrosa* sp.

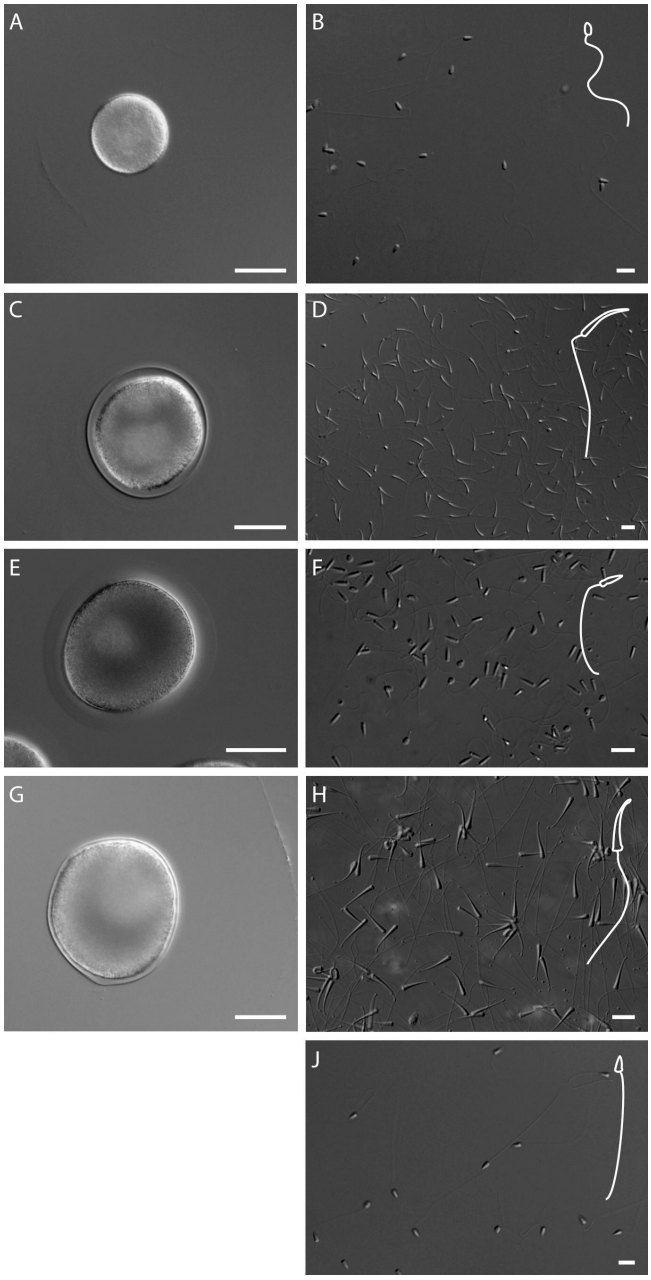

Fig. 3. Primary oocytes and sperm dissected from the members in *Maculaura* gen. nov. **(A, B)** *Maculaura alaskensis* comb. nov., **(C, D)** *Maculaura cerebrosa* sp. nov., **(E, F)** *Maculaura aquilonia* sp. nov., **(G, H)** *Maculaura magna* sp. nov., **(J)** *Maculaura oregonensis* sp. nov. Scale bars: 50 μm (A, C, E, G), 10 μm (B, D, F, H, J).

nov. in body shape, color, and size. *Maculaura alaskensis* differs from *M. cerebrosa* by having cerebral ganglia of the same general hue as the body (as opposed to having a distinctly pink brain) and a relatively longer caudal cirrus with an abrupt (as opposed to gradual) transition from posterior body (compare Fig. 4B with 4J). Differentiating *M. alaskensis* from *M. aquilonia* is challenging and best achieved with freshly collected specimens, as colors can fade in the lab over time. Whereas *M. alaskensis* is pale anteriorly, *M. aquilonia* can have a brownish region near the brain (Fig. 4F). The easiest way to distinguish *M. alaskensis* from *M. aquilonia* and the other three species is by comparing their eggs and sperm (Fig. 3). At 75 μm in diameter, *M. alaskensis* eggs are the smallest in the genus (*M. oregonensis* egg size is not known), and they lack a chorion. *Maculaura alaskensis* sperm is primitive with a short (5 μm) headpiece, similar to that in *M. oregonensis*, but distinctly different from the sperm in the other three species, which have variously elongated headpieces.

Habitat, type locality, and distribution. The known range of this species confirmed by DNA sequences extends from False Bay, San Juan Island, Washington to southern Oregon (WA-F1 to OR-C, Fig. 1A), where it is common. Individuals are commonly encountered in the top 10–15 cm of silty, relatively small-grained sand and mud from mid- to low intertidal (e.g. Fig. 1D) in protected bays and estuaries. Although patchy in distribution, several individuals can be found in one shovel-load, stretched like threads between clods and clumps of sand (Fig. 1E). It is quite possible that this species occurs further north and south along the Pacific coast of North America (including Alaska), but none of the individuals from outside Oregon and Washington, that we have sequenced, belong to this species. Coe (1901) did not specify a type locality, but based his description on specimens from a variety of locations in Alaska. Later, Coe (1904, 1940) revised the species range to include southern California and Mexico. The type locality of *M. alaskensis* comb. nov. is now regarded to be Charleston, OR, as the place of origin of the neotype becomes the type locality of the nominal species-group taxon, according to Article 76.3 of the Code (ICZN, 1999).

Description. *External appearance.* Largest specimens examined by us were 5 cm in length and 2–3 mm in width, with average length 3–4 cm and width 1–2 mm (Figs. 2B, 4A, B), while gliding. Living worms are, generally, a uniform pinkish or flesh-color. Body is rounded in the foregut region and dorso-ventrally flattened in the midgut region. Sexually mature individuals can appear pale yellow to white due to the color of gametes visible through the body wall between intestinal diverticula. The ventral surface is only slightly lighter than dorsal, if at all. The tip of the head is narrow and rounded, and head is not prominently demarcated from body when worm is gliding. Relatively shallow horizontal cephalic slits extend from anterior tip of the head to about the anterior margin of the mouth. Ocelli are lacking. Mouth is slit-like and elongated. The caudal cirrus is abruptly demarcated from the posterior end of body, and tends to be relatively long and thin compared to that in several other members of the genus (e.g. compare Figs. 2B with 2D, E, and 4B with 4J). Movement is without distinct peristalsis (Fig. 4A). Worms fragment during collection, especially when sexually mature, and posterior end regenerates routinely; anterior regeneration has not been observed. To avoid fragmentation worms should be collected with clumps of sand or mud, and cleaned in the laboratory.

Body wall. The epidermis is ciliated and of uniform thickness, situated on top of a thin dermis; the latter term used here in reference to the thin layer of extracellular matrix underlying the epidermis (Fig. 5E). Gland cells, staining red and blue, are interspersed within the cutis (subepidermal glandular region between the dermis and outer longitudinal musculature, OLM) (Fig. 5A–D). The transition from

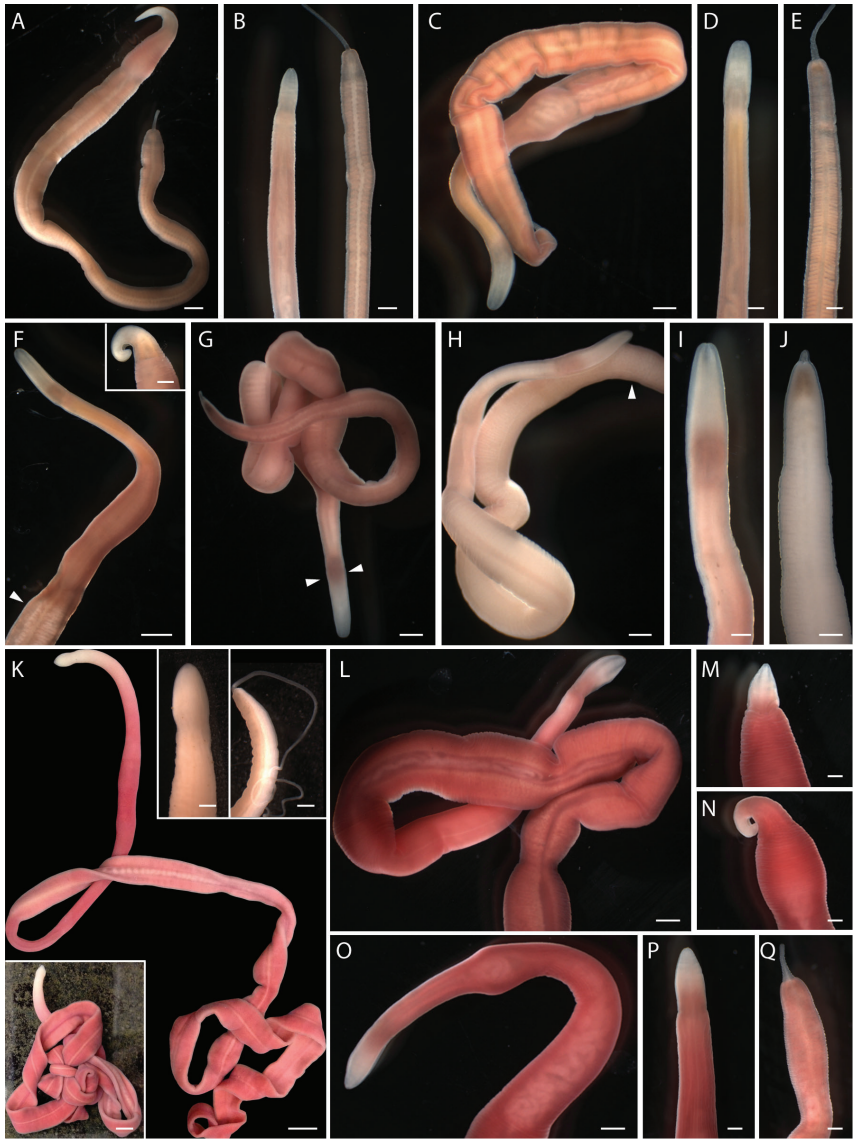

Fig. 4. External appearance of live adults in *Maculaura* gen. nov. **(A, B)** *Maculaura alaskensis* (Coe, 1901) comb. nov.: **(A)** entire body of non-type specimen; **(B)** anterior and posterior ends of same individual as (A), relaxed in $MgCl_2$. **(C–F)** *Maculaura aquilonia* sp. nov., two different specimens: **(C)** paratype, entire body; **(D)** magnification of head, same individual as (C), relaxed in $MgCl_2$; **(E)** magnification of tail, same individual as (C), relaxed in $MgCl_2$; **(F)** reproductive male (topogenetype specimen) with testes visible through the body wall (arrowhead), with magnification of head in upper-right inset. **(G–J)** *Maculaura cerebrosa* sp. nov.: **(G)** non-type specimen, showing the distinctly pink brain (indicated by arrowheads); **(H)** reproductive female (non-type specimen) with ovaries (indicated by arrowhead) visible through the body wall; **(I)** head of a relaxed (topogenetype) individual; **(J)** tail, same individual as (I). **(K)** *Maculaura magna* sp. nov., body of holotype and close-up of anterior and posterior of the same individual after relaxation in $MgCl_2$ (upper right insets); the background has been removed using Adobe Photoshop to emphasize the body color; bottom left inset shows the same individual on original background. **(L–Q)** *Maculaura oregonensis* sp. nov.: **(L–O)** body and anterior of holotype; note coiled proboscis visible through the anterior body wall (O); **(P–Q)** anterior and posterior of relaxed individual. Scale bars: 5.0 mm (K and left inset), 1.0 mm (A, C, F, G, H, K, L, O), and 0.5 mm (B, D, E, F inset, I, J, K insets, M, N, P, Q). Topogenetypes are associated with specimens pictured in F, I, J.

cutis to the OLM is gradual and visible only by the presence of gland cells that are confined to the cutis anteriorly and extend into the OLM immediately anterior and posterior to the mouth (compare Fig. 5A with 5C, E). The OLM is slightly thinner than the inner longitudinal muscle layer (ILM, e.g. Fig. 5E), but the two layers are of equal thickness in the intestinal region where the circular musculature (CM) is thickest (Fig. 5F). The thick esophageal circular muscle layer (1/2 as thick as body wall CM reported by Coe (1901) was not observed.

Proboscis and rhynchocoel. The rhynchocoel opening is slightly subterminal (ventral); proboscis is long and coiled. The rhynchocoel musculature under the vascular plug is not interwoven with body wall musculature. The proboscis consists of four distinct muscle layers including inner (endothelial) circular, longitudinal, diagonal, and outer circular; two thin muscle crosses were observed in confocal sections (A. Chernyshev, personal communication). The proboscis epithelium sits atop a thin layer of extracellular matrix; glandular ridge present and with red-staining gland cells (Fig. 5E, H).

Digestive system. The mouth is situated ventrally. The opening is a short (80 μm), thin slit that begins immediately posterior to the cephalic slits. Just anterior to the mouth opening, gland cells that open into the foregut ("accessory buccal glands", following Coe's terminology), become apparent ventrally (Fig. 5D) and remain prominent throughout the anterior esophageal region. At least two types of gland cells are associated with foregut epithelium, one staining orange-red and the other staining purple, and, at times, their bodies may extend into the OLM (Fig. 5D). The foregut is densely ciliated, folded and packed with gland cells. The transition from foregut to intestine is gradual. Intestinal diverticula are not branched. Short, unbranched hindgut opens via a ventral anus anterior to the caudal cirrus.

Excretory system. Relatively large nephridia are found 5 mm from the anterior tip (Fig. 5E) and extend as canals before opening to the outside via two dorso-lateral nephridiopores, one on each side (Fig. 5G) near the transition between foregut and intestine.

Vascular system. Two conspicuous lateral blood vessels flank the rhynchocoel, and a dorsal blood vessel is situated within the ventral wall of the rhynchocoel for the length of the foregut. The mid-dorsal blood vessel enters the rhynchocoel near the brain and forms a single ventral vascular plug. Two lateral cephalic blood lacunae are connected anteriorly via an anastomosing lacuna and, at the level of the brain com-

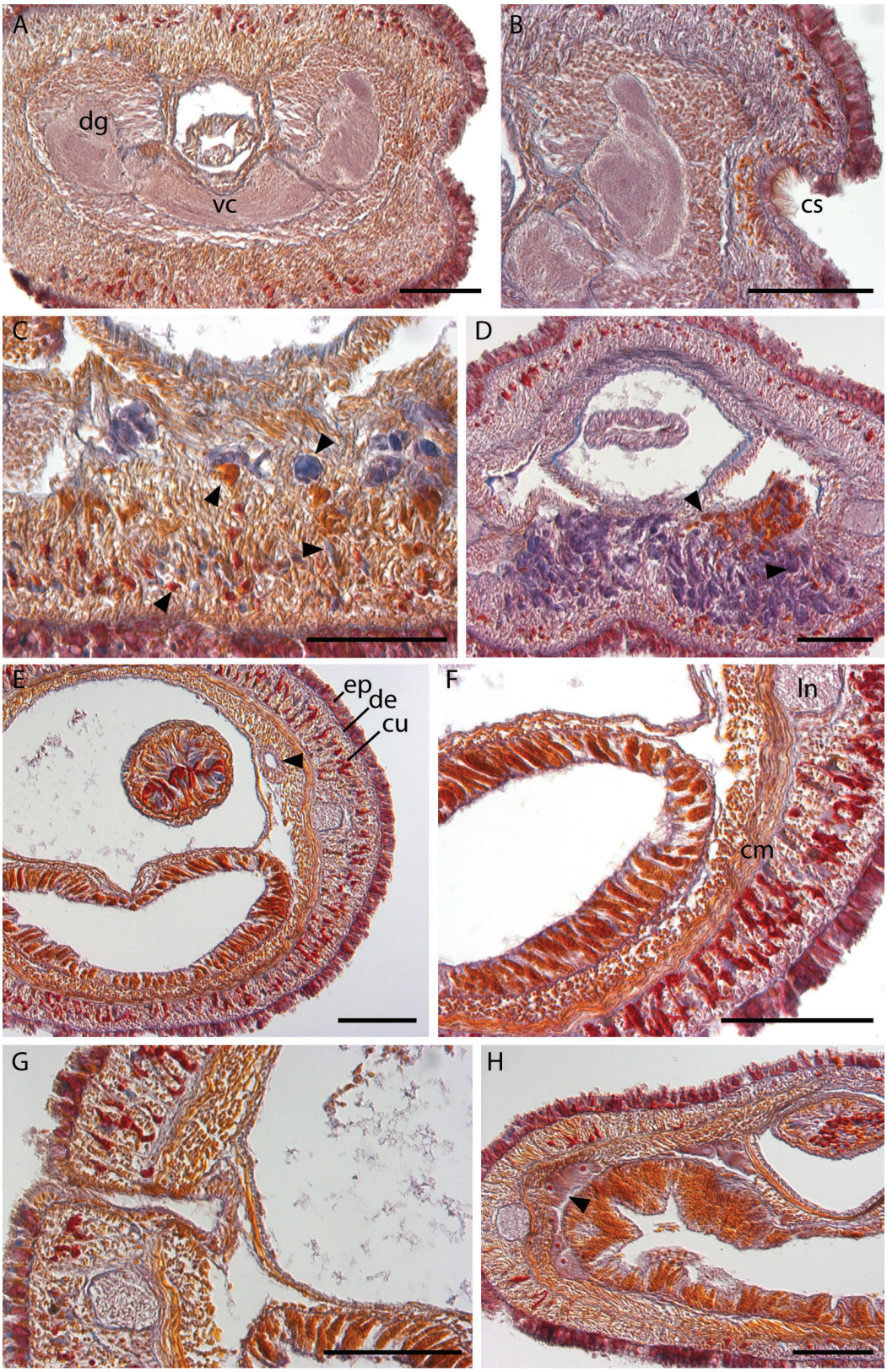

Fig. 5. *Maculaura alaskensis* (Coe, 1901) comb. nov., # 1282106 (neotype specimen), photomicrographs of transverse sections: **(A)** brain; **(B)** left cephalic slit; **(C, D)** gland cells in ventral longitudinal musculature anterior to mouth opening; note four distinct gland cell types, two in the cutis and two foregut (arrowheads, C); **(E)** nephridial collecting tubule (arrowhead) in intestinal region; **(F)** body-wall inner circular muscle layer in intestinal region; **(G)** nephridiocanal; **(H)** ovary; note several oocytes and nuclei (arrowhead). Abbreviations: **cm**, circular musculature; **cu**, cutis; **de**, dermis; **dg**, dorsal ganglion; **ep**, epidermis; **ln**, lateral nerve; **vc**, ventral commissure. Scale bars: 100 μm.

missures, surround the ventral rhynchocoel. These blood lacunae are, at times, connected with the blood sinuses surrounding the foregut and become distinct vessels posteriorly. The dorsal blood vessel originates from the commissure between the two lateral vessels just posterior to the ventral brain commissure and is easily observed ventral to the rhynchocoel wall in the intestinal region.

Nervous system. Dorsal and ventral cerebral ganglia are connected via dorsal and ventral commissures, respectively, surrounding the anterior rhynchocoel. The brain is relatively large, and the ventral commissure (Fig. 5A) is nearly twice as thick as the dorsal commissure. The proboscis has two lateral nerves clearly visible anteriorly, which arise from and enter the proboscis anterior to the ventral brain commissure. Lateral nerve chords are situated just outside the CM (Fig. 5F) and consist of a fibrous core and ganglionic region, which are surrounded by blue-staining inner and outer neurilemma, respectively. Two esophageal nerves originate from the inner margin of ventral cerebral lobes at the level of the cerebral organs and are apparent lateral and ventral of the main lateral nerves.

Sense organs. Paired cerebral organs lie just posterior to ventral brain commissure and their canals open into lateral cephalic slits (Fig. 5B). The epithelium of each cerebral organ canal is densely ciliated with underlying conspicuous gland and nerve cells staining orange and fuchsia, respectively (Fig. 5B). Each cerebral organ is connected to the dorsal cerebral ganglion via a cerebral organ nerve. Three apical sense organs were observed in confocal sections (A. Chernyshev, personal communication), but were not observed with histological sections.

Reproduction and development. Reproductive females and males have been collected March–September in OR and WA, with ripest individuals found in summer months. Gonads are arranged laterally between intestinal diverticula. Ovaries contain dozens of oocytes (Fig. 5H). Once dissected into seawater and rounded up, oocytes are 75 μm in diameter and without a chorion (Fig. 3A, Maslakova, 2010). Sperm head pieces (Fig. 3B, Maslakova, 2010) are 5-μm long, cone-shaped i.e. not modified (Stricker and Folsom, 1998). The wild-caught larva, identified as belonging to this species by DNA sequence data, was collected from Coos Bay plankton in October (Fig. 1C). When reared in the lab, first and second cleavage occurs at 2 and 3 hours after fertilization, respectively, at 11–14°C and larvae begin feeding on *Rhodomonas lens* at 3 days (Maslakova, 2010). They have three pairs of imaginal discs as early as 14 days, and the discs fuse to form a complete juvenile worm by as early as 28 days (Maslakova, 2010). Metamorphosis has been observed in lab culture as early as 35 days after fertilization. Prior to metamorphosis larvae are approximately 500 μm tall and wide (Maslakova, 2010). The larva exhibits the characteristic *pilidium maculosum* morphotype (Fig. 6), where the amnion surrounding the juvenile worm is pigmented with a polka-dot pattern consisting of red, black, and maroon pigment spots (Maslakova, 2010).

Maculaura aquilonia sp. nov.
(Figs. 2C, 3E–F, 4C–F, 7A–D, 8, 9)

Etymology. This specific epithet is a Latin adjective (*aquilonius*, *-a*, *-um*; "northerly" or "northern"), in reference to the geographic range of this species, reaching the northernmost latitudes for this genus.

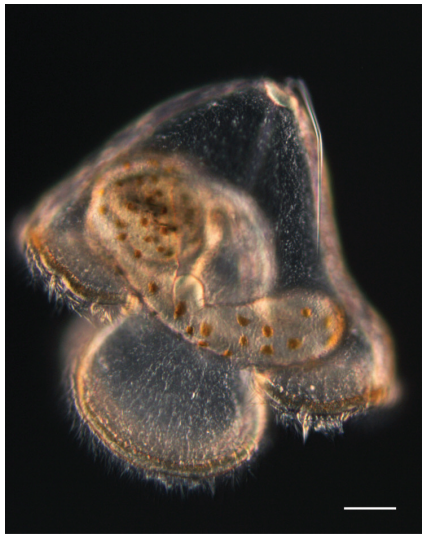

Fig. 6. Larva of *Maculaura alaskensis* (Coe, 1901) comb. nov., wild-caught from plankton sample taken 13 October 2013 from Coos Bay (diamonds, Fig. 1C) and identified using DNA sequence data. Scale bar: 100 μm.

Type material. Type material is deposited at the NMNH and includes serial transverse sections of the holotype (male, 20 slides # 1282112) and one paratype (18 slides # 1282113) as well as additional ethanol-preserved tissue. Additional paratypes include four un-sectioned paratypes preserved for histology (#s 1282114–12821117) and associated ethanol-preserved tissue (Table 1). We designate a partial COI sequence from an individual collected from Charleston, OR as a topogenetype (GenBank accession number KP682130, Table 1); ethanol-preserved tissue from this individual is also deposited at NMNH (# 1282118).

Material examined. Forty-three adult individuals, including holotype and paratypes, and four wild-caught larvae were examined and their identification confirmed by DNA sequence data. These individuals were collected from locations near Juneau, AK, and Charleston, OR, USA, as well as from the Sea of Okhotsk near Magadan, Russia (Table 1). COI sequence data from seven individuals collected in Kachemak Bay, AK, by S. Maslakova and J. Norenburg were supplied by J. Norenburg (Smithsonian Institute) from archived specimens (Table 1). Ethanol-preserved tissue and/or extracted DNA from remaining individuals are held at the OIMB.

Diagnosis. *Maculaura aquilonia* differs from *M. magna* and *M. oregonensis* by its smaller size, narrower body, and not as pink body color. It is similar to *M. alaskensis* and *M. cerebrosa* in body shape, color, and size. *Maculaura aquilonia* differs from *M. cerebrosa* by having cerebral ganglia of the same general hue as the body (Fig. 4C, D) (as opposed to having a distinctly pink brain, Fig. 4G, I) and a relatively longer caudal cirrus with an abrupt (Figs. 2C, 4E) (as opposed to gradual, Figs. 2D, 4J) transition from posterior body. *Maculaura aquilonia* can be differentiated from *M. alaskensis* by the presence of a subtle brownish region near

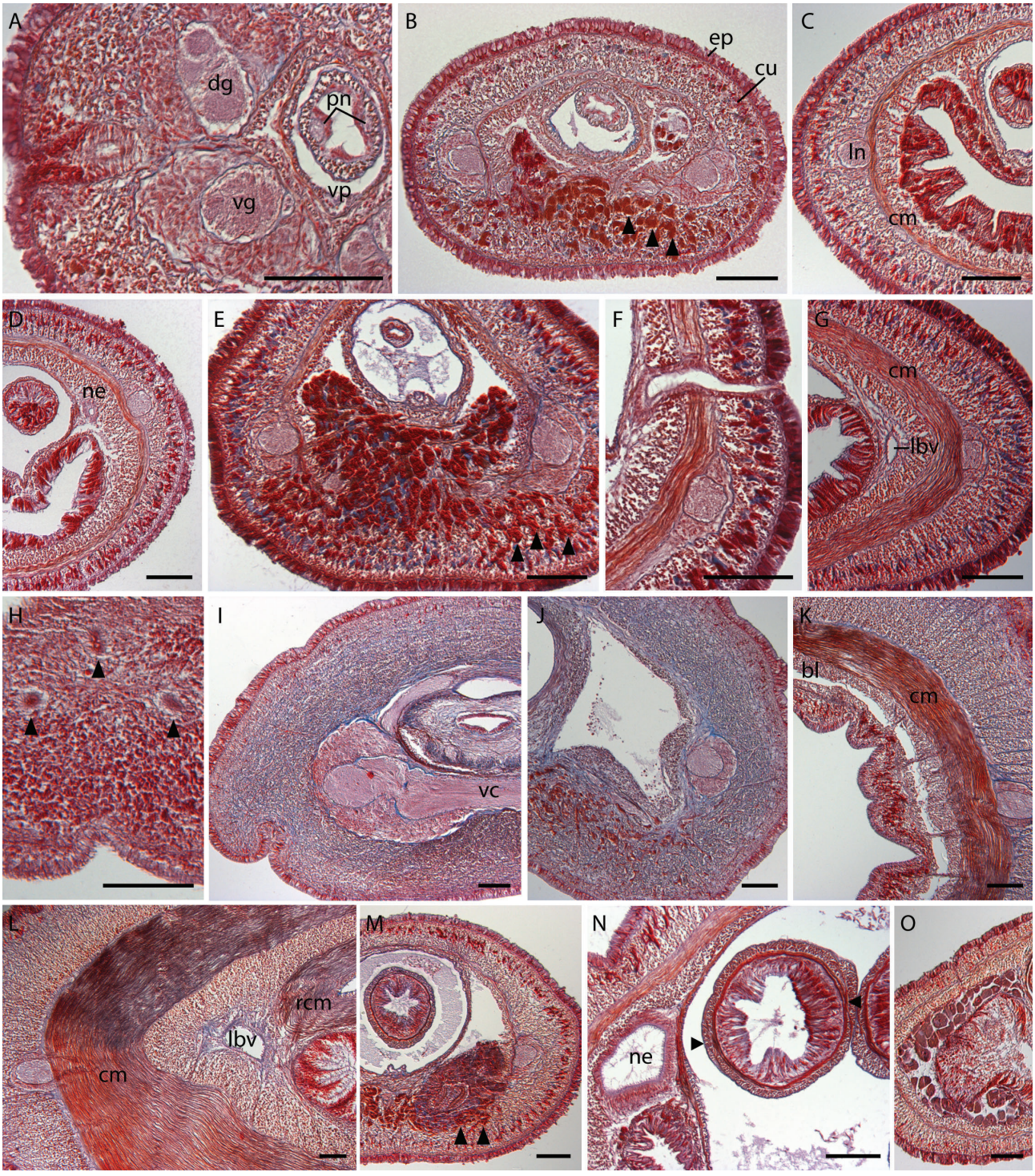

Fig. 7. Internal anatomy of *Maculaura* gen. nov. **(A–D)** *Maculaura aquilonia* sp. nov., USNM# 1282112 (holotype): **(A)** right cerebral organ and cerebral ganglia, proboscis, and rhynchocoel; **(B)** anterior to mouth opening, showing ventral gland cells (arrowheads); **(C)** foregut region; **(D)** intestinal region. **(E–G)** *Maculaura cerebrosa* sp. nov., USNM# 1282119 (holotype): **(E)** anterior to mouth opening, showing ventral gland cells (arrowheads); **(F)** left dorsolateral nephridiocanal and pore; **(G)** posterior intestinal region. **(H–L)** *Maculaura magna* sp. nov., USNM# 1282125 (holotype): **(H)** apical sense organs (arrowheads); **(I)** ventral cerebral commissure; **(J)** anterior to mouth opening; **(K)** posterior to mouth opening; **(L)** mid intestinal region, showing extremely thick circular musculature. **(M–O)** *Maculaura oregonensis* sp. nov., USNM# 1282128 (holotype): **(M)** anterior to mouth opening, showing ventral gland cells (arrowheads); **(N)** intestinal region, showing two proboscis muscle crosses (arrowheads); **(O)** ovary. Abbreviations: **bl**, blood lacunae; **cm**, circular musculature; **cu**, cutis; **dg**, dorsal ganglion; **ep**, epidermis; **lbv**, lateral blood vessel; **ln**, lateral nerve; **ne**, nephridium; **pn**, proboscis nerves; **rcm**, rhynchocoel circular musculature; **vc**, ventral commissure; **vg**, ventral ganglion; **vp**, vascular plug. Scale bars: 100 μm.

the brain, which is best observed in freshly collected specimens (Fig. 4C, D, F). We observed this color in the majority of freshly collected specimens, and it seemed to fade over time in the lab. The most accurate way to differentiate *M. aquilonia* from *M. alaskensis* and the other three species is by comparing their eggs and sperm (Fig. 3). *Maculaura alaskensis* eggs are the smallest in the genus (*M. oregonensis* egg size is not known), and they lack a chorion (Fig. 3A). The eggs of *M. aquilonia* also lack a chorion, but are larger, 90–100 μm in diameter (Fig. 3E). *M. alaskensis* sperm is primitive with a short (5 μm) headpiece (Fig. 3B). *Maculaura aquilonia* and *M. oregonensis* sperm are indistinguishable, they both have slightly elongated but not curved headpieces 7–8 μm in length (Fig. 3F, J). In comparison, the sperm headpieces of *M. cerebrosa* and *M. magna* are longer (10–15 μm) and slightly curved. *Maculaura aquilonia* can also be differentiated from the latter two species by body color; it is not as pink (compare Fig. 4C with 4L–Q).

Habitat, type locality, and distribution. Type locality is in Juneau, AK (58.3952°N, 134.7512°W) (AK-J1, Fig. 1B). This species exhibits the largest confirmed range for any species in the genus *Maculaura*, including eastern Russia, Alaska, and southern Oregon (RU-O1, AK-K1 to OR-C, Fig. 1A). This species is common in silty sand and mud from mid- to low intertidal, sometimes even occurring in black anoxic mud. However, in Juneau, AK, it is found under rocks and within fine mud, where it appears to be the most common nemertean species. In the southern portion of its range, this species is less common than the morphologically similar *M. alaskensis* and was most abundant at one mudflat along the South Slough estuary near Charleston, OR (OR-C10, Fig. 1C).

Description. *External features.* Largest specimens were 5 cm in length and 2–3 mm in width, with average individuals on the order of 3–4 cm and 1–2 mm, in gliding (Fig. 4C–F). Head is off-white and body color is pale yellowish pink to brownish ochre. Posterior can be very pale yellow to off-white in reproductive individuals where gametes are seen through the body wall (Fig. 4F). Body color is the same dorsally and ventrally. Lightly colored brownish pigment near the brain can be seen through the anterior body wall in freshly collected specimens (Fig. 4F). The posterior-most region of the body transitions abruptly to the caudal cirrus (Fig. 4E). Movement is without distinct peristalsis and is led with the head, which often turns dramatically to one side forming a hook or 'U-shape' (Fig. 4C, F inset). Fragmentation occurs during collection, especially in sexually mature individuals; posterior end regenerates routinely. Individuals can be rather short and stout when ripe with gametes. External morphology is very similar and sometimes indistinguishable from *M. alaskensis* (compare Fig. 4A with 4C).

Internal features. Internal anatomy as in *M. alaskensis* (see Fig. 7A–D).

Reproduction and development. Sexes are separate. Gonads are regularly arranged between intestinal diverticula (Fig. 4F). Reproductive individuals have been collected in March 2013 in southern Oregon. Gametes from both sexes are released when ripe through serially arranged dorsolateral gonopores. Dissected primary oocytes are 90–100 μm in diameter and lack a chorion (Fig. 3E). Sperm headpiece is cone-shaped, 7.5 μm in length (n = 10, Fig. 3F). Wild-caught larvae identified as belonging to this species using DNA sequence data were collected from plankton in Coos Bay in April and May in 2009 and 2012 (Fig. 1C). The amnion surrounding the juvenile worm inside the larva is less pigmented in this species as compared to the others in this genus (Fig. 8). However, we observed pigment spots in the amnion of lab-reared larvae during and immediately following metamorphosis, when the amnion collapses and is swallowed by the juvenile (Fig. 9). When reared in the lab at 12°C, first and second cleavage occur at approximately two and three hours after fertilization, respectively, and larvae begin feeding on *Rhodomonas lens* at 2 days (Fig. 8A). Pilidia have three pairs of imaginal discs by 2.5 weeks and the trunk and cerebral organ discs fuse by 42 days (Fig. 8C). The larvae reach advanced-proboscis stage by 81 days (Fig. 8D), and metamorphosis was observed as early as 95 days. Metamorphically competent larvae are approximately 550 μm tall (Figs. 8E, F). Metamorphosis is catastrophic, as in other pilidia, and the juvenile nemertean ingests the larval body (Fig. 9).

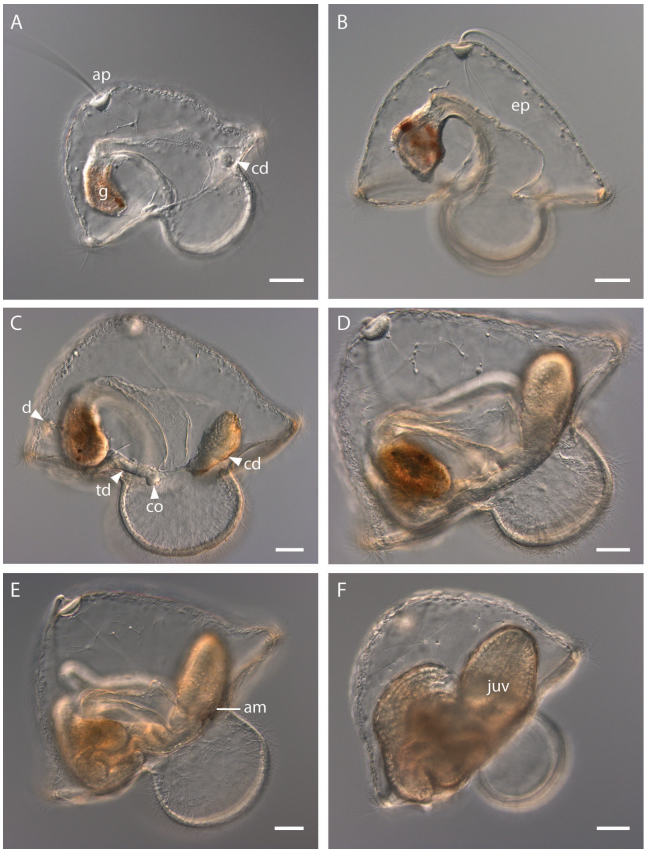

Fig. 8. Development in *Maculaura aquilonia* sp. nov. **(A)** Two-day-old larva with cephalic disc in focus and gut positioned at left. **(B)** An 11-day-old larva. **(C)** Forty-two-day old larva with trunk discs and cerebral organ discs fused; the unpaired dorsal rudiment is also visible. **(D–F)** Larvae with juvenile; **(D)** 81-day old larva; **(E)** 91-day old larva; **(F)** 95-day old larva. Abbreviations: **am**, amnion; **ap**, apical tuft; **cd**, cephalic disc; **co**, cerebral organ disc; **d**, dorsal disc (unpaired); **ep**, episphere; **g**, gut; **juv**, juvenile; **td**, trunk disc. Scale bars 100 μm.

Maculaura cerebrosa sp. nov.
(Figs. 2D, 3C–D, 4G–J, 7E–G, 10)

Etymology. The specific name is a compound unorthodox adjective (*cerebrosus*, *-a*, *-um*) rather freely formed by fusing two Latin words (*cerebrum* = brain, *roseus* = pink), in reference to the pinkish brain.

Type material. Serial transverse sections of the holotype (ripe male, 37 slides # 1282119), four paratypes (#s 1282120–1282123) and associated ethanol-preserved tissue are deposited at the NMNH (Table 1). We designate a partial COI sequence from an individual collected in Charleston, OR as a topogenetype (GenBank accession number KP682146, Table 1) and ethanol-preserved tissue from this individual is also deposited at NMNH (# 1282124).

Material examined. Fourteen adult individuals, including holotype and paratypes, and three wild-caught larvae were examined and their identification confirmed by DNA sequence data. These individuals were collected from locations near Charleston, OR, and Crescent City, CA (Table 1). Ethanol-preserved tissue and/or extracted DNA from remaining individuals are held at the OIMB.

Diagnosis. *Maculaura cerebrosa* differs from *M. magna* and *M. oregonensis* by its smaller size, narrower body, and not as pink body color. It is morphologically similar to *M. alaskensis* and *M. aquilonia* in body shape, color, and size. *Maculaura cerebrosa* is distinguishable from the latter two species by having a distinctly pink brain, which is visible through the body wall, and a short caudal cirrus with gradual (as opposed to a relatively longer caudal cirrus with an abrupt) transition from posterior body (Figs. 2D, 4G–J). In addition to the conspicuous pink brain, *M. cerebrosa* can be differentiated from *M. alaskensis* and *M. aquilonia* by comparing their eggs and sperm (Fig. 3). The eggs of *M. cerebrosa* and *M. magna* are both surrounded by egg chorions (the eggs of *M. oregonensis* have not been observed), but the egg diameter is distinctly different: 95 μm in *M. cerebrosa* and 125 μm in *M. magna* (compare Fig. 3C with 3G). The sperm headpieces in both species are elongated, but are 10 μm long in *M. cerebrosa* and 15 μm long in *M. magna* (Fig. 3D and 3H). The remaining species (for which we know gamete morphology) have eggs without distinct chorions, and "primitive" (not elongated) sperm (see Fig. 3).

Habitat, type locality, and distribution. The type locality is a mudflat near the outer Boat Basin in Charleston, OR (43.3445°N, 124.3215°W) (OR-C15, Fig. 1C). The known range of this species confirmed by DNA sequences extends from southern Oregon to northern California (OR-C to CA-C1, Fig. 1A), although a larger range is expected. This species can co-occur with other members in this genus, particularly *M. alaskensis*; however, *M. cerebrosa* is more common under rocks in mid-intertidal gravel and shell hash rather than sand. Individuals are often found intertwined under small rocks along the edges of mudflats (as in Coos Bay, OR or Crescent City, CA) or on the open coast in shell hash and amongst the roots of *Phyllospadix* sp. (e.g. in Sunset Bay, Middle Cove, South Cove, and North Cove at Cape Arago, OR).

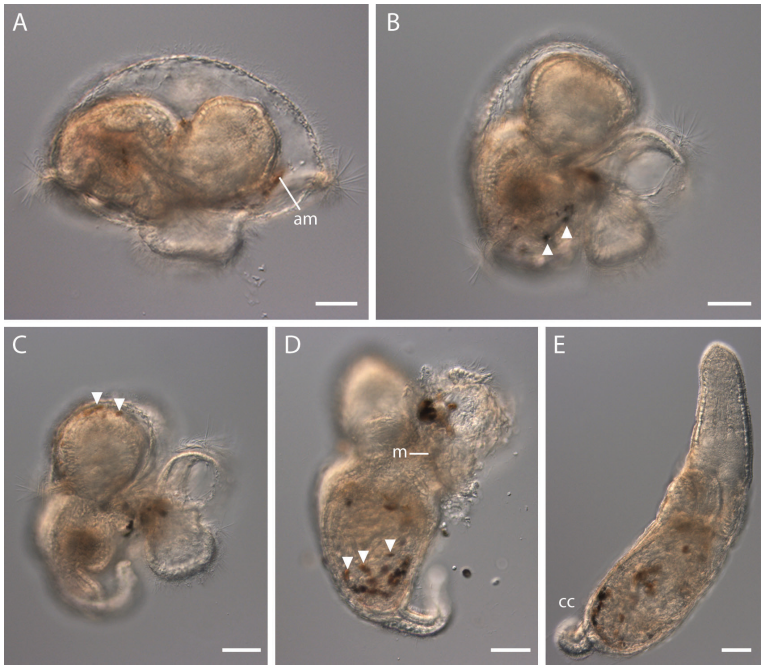

Fig. 9. Metamorphosis in *Maculaura aquilonia* sp. nov. **(A–E)** Pigment spots on the amnion (am) become apparent as the amnion disappears into the juvenile mouth (m) and collapses within the gut (arrowheads, B–D); (E) newly metamorphosed juvenile with caudal cirrus (cc). Scale bars: 100 μm.

Description. *External features.* Overall body and head shape as in *M. alaskensis* and *M. aquilonia*, but reaching greater lengths than either species. Largest specimens are 10 cm in length and 3–4 mm in width, with average individuals on the order of 5 cm long and 2 mm wide (Fig. 4G–J), while gliding. Head is narrow anteriorly and not prominently demarcated from body when worm is gliding (Fig. 2D). Head shape changes dramatically when contracted, at which time the head tip can be rather pointed. Body is generally a pale pink, rounded anteriorly and dorso-ventrally flattened posteriorly. The posterior of reproductive individuals can be pale pink to yellow, and gametes are visible through the body wall (Fig. 4H). Ventral surface of body slightly lighter colored than dorsal. The most notable exterior feature in this species is a conspicuous pink or rose pigment of the brain (Fig. 4G–I). Caudal cirrus is distinct from those of the other species in the genus as it is rather short and gradually tapers from posterior of body instead of transitioning abruptly, e.g. as in *M. alaskensis* and *M. aquilonia* (cf. Fig. 4B, E, J). Movement is without distinct peristalsis and is led with the head, which can contract and taper dramatically. Individuals often seek out and attempt to burrow under objects in glass bowls (e.g. rulers, rocks). Fragmentation occurs during collection, especially in sexually mature individuals, and posterior end regenerates routinely as in *M. alaskensis* and *M. aquilonia*.

Internal features. Internal anatomy as in *M. alaskensis*. (see Fig. 7E–G).

Reproduction and development. Sexes are separate. Reproductive females and males have been collected March through October, with sexually mature individuals mostly found in spring months, slightly earlier than is seen in

Maculaura alaskensis. Gametes are arranged serially between intestinal diverticula, as in other *Maculaura* species. Dissected oocytes are 95 μm in diameter (n = 10) and surrounded by a chorion (Fig. 3C). Sperm headpiece is shaped like the blade of an agricultural scythe and is 10 μm in length (Fig. 3D).

When reared in the lab, first and second cleavage occurs at roughly two and three hours post fertilization (at 12°C), respectively, and larvae begin feeding on *Rhodomonas lens* at 2–3 days. The cephalic discs and trunk discs develop at approximately one week (Fig. 10A) and polka-dot pigment characteristic of the *pilidium maculosum* morphotype is apparent on the cephalic discs by 14 days (arrowhead, Fig. 10B). Larvae have all three pairs of imaginal discs as early as 18 days (Fig. 10C) and reach the torus stage (Maslakova, 2010) as early as 25 days (Fig. 10D). In a single cohort (fertilized in March 2014), metamorphosis was observed after approximately 45 days post-fertilization. Metamorphically competent larvae are approximately 500 μm from apical tuft to apex of lateral lappet (Fig. 10E). Metamorphosis is catastrophic, as in other pilidia, and the emerging juvenile devours the larval body. The amnion surrounding the juvenile worm is decorated with red, black, and maroon pigment spots (Fig. 10F). Wild-caught larvae, confirmed to belong to this species by DNA sequencing, were collected from plankton in Coos Bay in August.

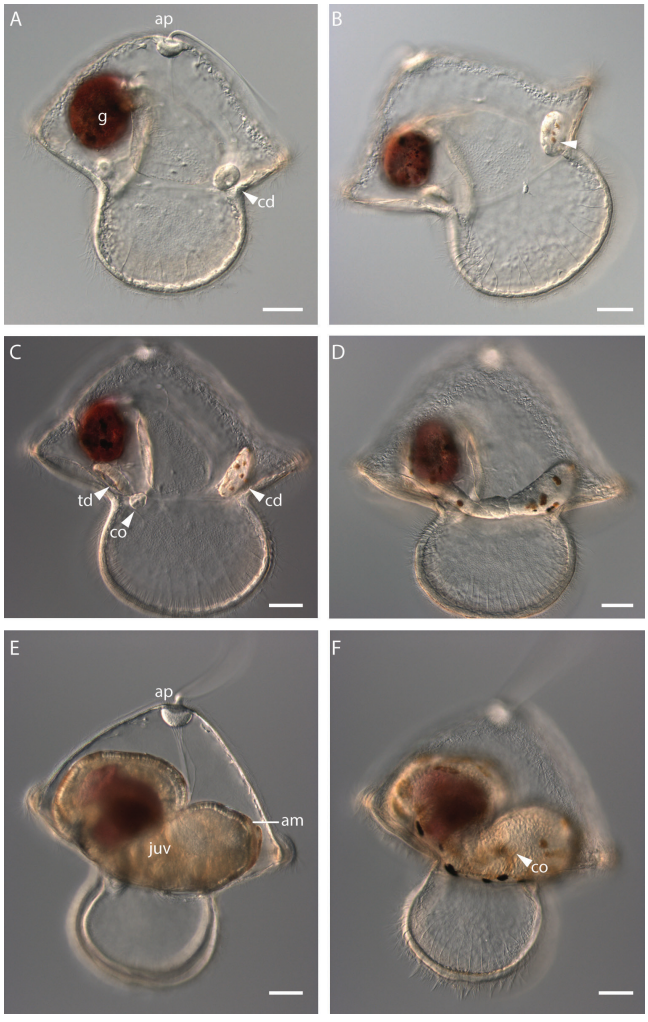

Fig. 10. Development in *Maculaura cerebrosa* sp. nov. **(A)** A nine-day-old larva with cephalic discs in focus and gut positioned at left. **(B)** Polka-dot pigment spots on cephalic discs present at 14 days (arrowhead). **(C)** An 18-day-old larva. **(D)** Twenty-five-day old larva with fused discs. **(E, F)** The juvenile nemertean surrounded by a pigmented amnion (in focus in F) and competent to metamorphose at approximately 45 days; note cerebral organs (F). Abbreviations: **cd**, cephalic disc; **co**, cerebral organ disc; **g**, gut; **juv**, juvenile; **td**, trunk disc. Scale bars: 100 μm.

Maculaura magna sp. nov.
(Figs. 2F, 3G–H, 4K, 7H–L, 11)

Etymology. This specific name is a Latin adjective (*magnus*, *-a*, *-um*; "great" or "large") in reference to the large size of this species, reaching sizes greater than any other known member of this genus.

Type material. Type material is deposited at NMNH and includes serial transverse sections of the holotype (56 slides # 1282125) and two un-sectioned paratypes preserved for histology and their associated ethanol-preserved tissue (#s 1282126–1282127) (Table 1). We designate a partial COI sequence derived from the holotype as a hologenetype (GenBank accession number KP682147, Table 1).

Material examined. Thirteen adult individuals, including the holotype and paratypes, and 18 wild-caught larvae were examined and in most cases their identification was confirmed by DNA sequence data. All individuals were collected from locations near Charleston, OR (Table 1). Two paratypes lack good quality DNA sequence data, but were confidently identified by morphology alone (#s 1282126–1282127). Ethanol-preserved tissue and/or extracted DNA from remaining individuals are held at the OIMB.

Diagnosis. *Maculaura magna* is the largest species in the genus (Fig. 2B–F). It differs from *M. alaskensis*, *M. aquilonia*, and *M. cerebrosa* by a pinkish-red body color (Fig. 4K). Internally the cutis of *M. magna* has fewer gland cells than in other members of this genus (Fig. 7I). *Maculaura magna* is morphologically most similar to *M. oregonensis* because both species have pink body color. However, *M. magna* is overall larger and its body is more of a dusty rose color compared to *M. oregonensis*, which is brighter pink or reddish (compare Fig. 4K with 4L–Q). The most accurate way to differentiate species in this genus is by comparing their eggs and sperm (Fig. 3). The eggs of *M. magna* are large (125 μm in diameter), surrounded by an egg chorion and sperm headpieces are elongated and 15 μm in length (Fig. 3G–H). The only other species that has gametes of similar morphology is *M. cerebrosa*; however, the gametes of *M. cerebrosa* are smaller than those of *M. magna.* The eggs of *M.cerebrosa* are 95 μm and sperm headpieces are 10 μm in length (compare Fig. 3G–H with 3C–D).

Habitat, type locality, and distribution. The type locality is a mudflat in Charleston, OR (43.3428°N, 124.3218°W) (OR-C1, Fig. 1C). This species is currently only known from southern OR where it is common in sand (e.g. Fig. 1D) and mud from mid to low intertidal. Single individuals are usually found, not occurring in groups, and they can be burrowed quite deep (to 0.75 m). We have found specimens in a vari-

ety of sandflats along the shores of Coos Bay, north to Empire, as well as along South Slough estuary near the Charleston Marina. Several individuals have been collected from a sandy beach at North Cove near Cape Arago, OR. However, at these locations it is not nearly as common as *M. alaskensis* or *M. cerebrosa*.

Description. *External features.* Resembles species of *Cerebratulus* in being rather large, broad, and dorso-ventrally flattened. Largest specimens are up to 30 cm in length and 1 cm in width, and average individuals are approximately 20 cm in length and 3–4 mm wide (Fig. 4K). Head is pale white and body can be rather dark pink (Fig. 4K bottom left inset), with a gradual transition in color from the anterior to posterior. The foregut region is rounded in cross-section, while the mid-body region is flattened dorso-ventrally (Fig. 2F), but rounded in individuals packed with gametes. Dorsal side can be somewhat darker than the ventral side in some individuals, with a sharp lateral transition between the dorsal and ventral color. Head can be pointed and change shape dramatically when contracted (Fig. 2F). The posterior region of the body ends abruptly with caudal cirrus (Figs. 2F inset, 4K upper right inset). Movement is with gentle peristalsis and is led with the head, which can curve from side to side. Fragmentation occurs frequently during collection in the field, due to the large size of this species. The posterior end regenerates easily, but slower than in smaller species (*M. alaskensis*, *M. aquilonia*, and *M. cerebrosa*), and anterior regeneration has not been observed. Regenerated region is typically lighter in color than adjacent (non-regenerated) body.

Internal features. Internal anatomy similar to *M. alaskensis* (see Fig. 7I–L). Three relatively large apical sense organs are clearly visible just anterior to the proboscis pore in histological sections (Fig. 7H). Mouth is ventral and quite long (up to 1 mm). Transition from foregut to intestinal region is met with a dramatic thickening of the circular musculature (Fig. 7L). The proboscis musculature exhibits two distinct crosses extending from the circular muscle to the proboscis endothelium. The diagonal proboscis muscle layer is thin and less conspicuous in *M. magna* than in the other four species. The proboscis also contains two outer longitudinal muscle strands outside the main proboscis nerves, which were not observed in the other four species. The nephridial canals are larger in this species than in other *Maculaura* species, as is, perhaps, fitting, since it is a larger species.

Reproduction and development. Sexes are separate. Ripe females were collected in June, and a reproductive male was collected in January 2012. Gametes are arranged laterally between intestinal diverticula. Dissected oocytes are 125 μm in diameter (n = 10), surrounded by a chorion (Fig. 3G). Sperm headpiece is elongated, 15 μm in length (Fig. 3H). Wild-caught larvae, confirmed to belong to this species by DNA sequence data, were collected from plankton in Coos Bay March through December and exhibit the *pilidium maculosum* morphotype (Fig. 11). The larval episphere is haystack-shaped and tall with relatively short lateral lappets (Fig. 11B, C).

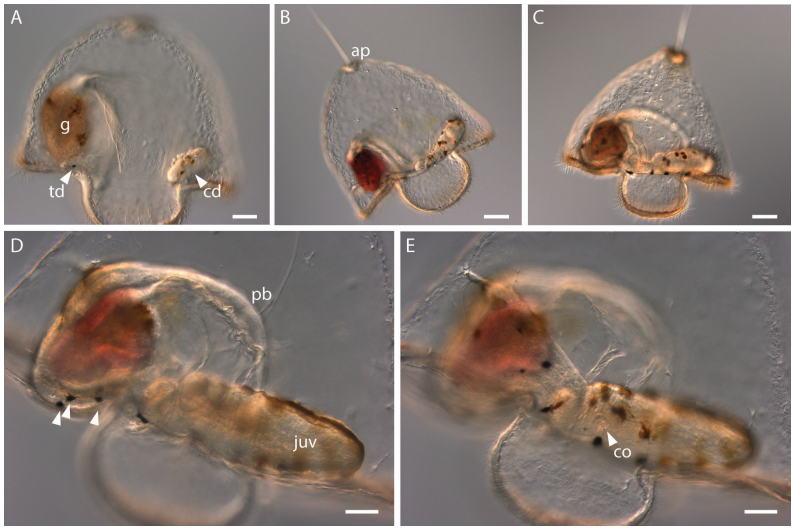

Fig. 11. Wild-caught larvae of *Maculaura magna* sp. nov. **(A)** Larva collected 2 July 2013; note polka-dot pigment spots on cephalic discs. **(B)** Larva collected 10 June 2013 with fused discs and apical tuft just out of focal plane. **(C–E)** Larva collected 1 July 2013 with advanced juvenile, proboscis rudiment, and pigment spots on amnion (D, arrowheads); a different focal plane shows the cerebral organ (E, arrowhead). Abbreviations: **ap**, apical tuft; **cd**, cephalic discs; **co**, cerebral organ; **g**, gut; **juv**, juvenile; **pb**, proboscis rudiment; **td**, trunk disc. Scale bars: 100 μm.

Maculaura oregonensis sp. nov.
(Figs. 2E, 3J, 4L–Q, 7M–O)

Etymology. The specific name is an adjective (*-ensis*, *-ense*), referring to the type locality and currently known distribution of this species.

Type material. Serial transverse sections of the holotype (female, 39 slides # 1282128), one paratype preserved for histology (# 1282129) and associated ethanol-preserved tissue are deposited at NMNH (Table 1). We designate a partial COI sequence from the holotype as a hologenetype (GenBank accession number KP682159, Table 1).

Material examined. Eleven adult individuals, (all collected from locations near Charleston, OR) including the holotype and paratype were examined and their identification confirmed by DNA sequence data (Table 1). Ethanol-preserved tissue and/or extracted DNA from remaining individuals are held at the OIMB.

Diagnosis. *Maculaura oregonensis* differs from *M. alaskensis*, *M. aquilonia*, and *M. cerebrosa* by its larger size, wider body, and pink body color. Internally, *M. oregonensis* differs from these three species further, in that more red and fewer blue staining gland cells are present in the cutis (compare Fig. 7E with 7M). External color in *M. oregonensis* most closely resembles *M. magna*; however, the latter species is significantly larger than *M. oregonensis* and the body color differs slightly between the two species. *Maculaura oregonensis* is bright pink or reddish in color while *M. magna* exhibits more of a dusty rose body color (compare Fig. 4K with 4L–Q). The sperm headpiece is shorter in *M. oregonensis* compared to that in *M. cerebrosa* and *M. magna*. The sperm of *M. oregonensis* has similar morphology to *M. alaskensis* but is slightly longer (compare Fig. 3B

with 3J). *Maculaura oregonensis* and *M. aquilonia* sperm are indistinguishable; they both have slightly elongated headpieces (although not as long as *M. cerebrosa* or *M. magna*) that are 7–8 μm in length. Instead, these species can be differentiated by body color alone, in that *M. oregonensis* is significantly darker pink (compare Fig. 4C with 4L–Q). At present we lack information on size and presence of the chorion in oocytes of *M. oregonensis.*

Habitat, type locality, and distribution. The type locality is a mudflat in Charleston, OR (43.3272°N, 124.3263°W) (OR-C10, Fig. 1C). This species is, at present, only found in southern Oregon where it is relatively rare. Individuals can be found in sand and mud from mid- to low intertidal (e.g. Fig. 1D). Several specimens were collected in north Coos Bay, near the McCullough Bridge, and few individuals were collected with other species of this genus at a variety of mudflats along the South Slough estuary (Fig. 1C). In one instance, several individuals were observed surrounding the hoplonemertean, *Paranemertes peregrina.*

Description. *External features*. Largest specimens were 15 cm in length and 5 mm in width, while gliding, with average individuals about 8–10 cm long and 3 mm wide (Fig. 4L–Q). Head is pale white and body color is dark pink. The dorsal side is the same color as ventral side. The body is rounded in cross-section anteriorly and dorso-ventrally flattened posteriorly. Head narrows to a point while worm is gliding (Fig. 4L–O). The proboscis is paler than the background color of the body and can easily be seen through the body wall (Fig. 4O). Brain is pink and shows through the body wall, as a somewhat darker pink at the transition from the pale color of the head to the bright pink of the body. Caudal cirrus present, somewhat intermediate in shape between that of *M. cerebrosa* and the other species in the genus (Figs. 2E, 4Q). Movement is with gentle peristalsis, as in *M. magna*, and is led with the head, which can curl dramatically (Fig. 4N). *Maculaura oregonensis* is often seen retracting its head within its body (Fig. 4M). Fragmentation occurs during collection and posterior end regenerates routinely, but anterior regeneration has not been observed.

Internal features. Internal anatomy as in *M. alaskensis* (see Fig. 7M–O). The two proboscis muscle crosses are most conspicuous in this species and the nephridia are comparatively larger than in *M. alaskensis, M. aquilonia* and *M. cerebrosa*, but smaller than *in M. magna* (Fig. 7N).

Reproduction and development. Sexes are separate. The gametes of one ripe male were observed on 20 May 2014 (Fig. 3J). Sperm headpiece is approximately 7–8 μm (n = 10) in length. Reproductive females were observed in the Summer 2014, but the size of the oocytes was not recorded. Each ovary of the holotype contained approximately 35 oocytes (Fig. 7O).

Phylogenetic analysis, haplotype networks, and species delimitation

Bayesian (not shown) and ML analyses (Fig. 12) of the 16S and COI datasets each resulted in five well-supported monophyletic clades, corresponding to the five species described here (Fig. 12). Consistently between different analyses, *M. alaskensis* and *M. oregonensis* were sister species; however, the relationships between the other three species differed depending on the gene region (compare Fig. 12A with 12B).

The average uncorrected intraspecific and interspecific percent divergence values are reported in Table 2. Four of the five species have intraspecific divergence values of < 1% for both 16S and COI gene regions (Table 2). *Maculaura magna* is an exception; it exhibits the largest intraspecific variation at 1.1% and 7.1% for the 16S and COI gene regions, respectively. A sufficient barcoding gap (Meyer and Paulay, 2005) exists, as the interspecific divergence between the two most closely related species, *M. oregonensis* and *M. alaskensis*, is 4.0% and 14.3% for the 16S and COI gene regions, respectively.

A similar barcoding gap was detected using ABGD: between 5% and 6% (16S) and between 3% and 7–9% (COI). For the 16S gene region, the four species *M. alaskensis*, *M. aquilonia*, *M. cerebrosa*, and *M. oregonensis* were corroborated in ABGD using a cut-off value of 1.3%; however, *M. magna,* the species that exhibits the greatest degree of sequence divergence, was divided into five groups (not shown). With a cut-off value from 2.2–6.0%, ABGD reveals four species *Maculaura magna*, *Maculaura cerebrosa*, *Maculaura aquilonia*, and a species composed of both *M. alaskensis* and *M. oregonensis* (Table 3). ABGD analysis of COI data (using cut off values from 1.7% to 10%) consistently found nine taxa (Table 3). *Maculaura alaskensis*, *M. cerebrosa*, and *M. oregonensis* were consistent with our previous delimitation; however, *M. magna* was partitioned into four species and *M. aquilonia* into two.

TCS networks were generated from the same alignments using a 95% confidence interval (Hart and Sunday, 2007) (Table 3). While analysis of 16S data revealed five networks that correspond to the five species described above, analysis of COI data revealed additional networks within *M. magna* (3 total) and *M. aquilonia* (2 total). Four of the five species show little intraspecific divergence with 10 or fewer haplotypes each (Fig. 13A–E). Haplotype networks for *M. cerebrosa* reveal three haplotypes, separated by one nucleotide change (Fig. 13C) and both *M. alaskensis* (Fig. 13A) and *M. aquilonia* (Fig. 13B) have 10 haplotypes each. *M. oregonensis* has four haplotypes, separated by 1–5 nucleotide changes (Fig. 13D) and *M. magna* has eight 16S haplotypes separated by the largest number of nucleotide differences observed in these five species (Fig. 13E).

TCS analysis of COI data reveals a single haplotype network for each of three species (*M. alaskensis*, *M. cerebrosa*,

Table 2. Inter- and intraspecific variation shown as uncorrected *p*-distances for 16S rDNA and COI (bold text) gene regions.

	M. alaskensis	*M. aquilonia*	*M. cerebrosa*	*M. magna*	*M. oregonensis*
Maculaura alaskensis	0.2	10.9	11.2	10.5	4.0
	0.7	**17.9**	**17.4**	**17.0**	**14.3**
Maculaura aquilonia		0.1	8.8	8.0	12.2
		0.3	**14.8**	**13.9**	**16.3**
Maculaura cerebrosa			0.1	10.2	11.7
			0.6	**12.9**	**18.0**
Maculaura magna				1.1	11.0
				7.1	**16.3**
Maculaura oregonensis					0.4
					0.2

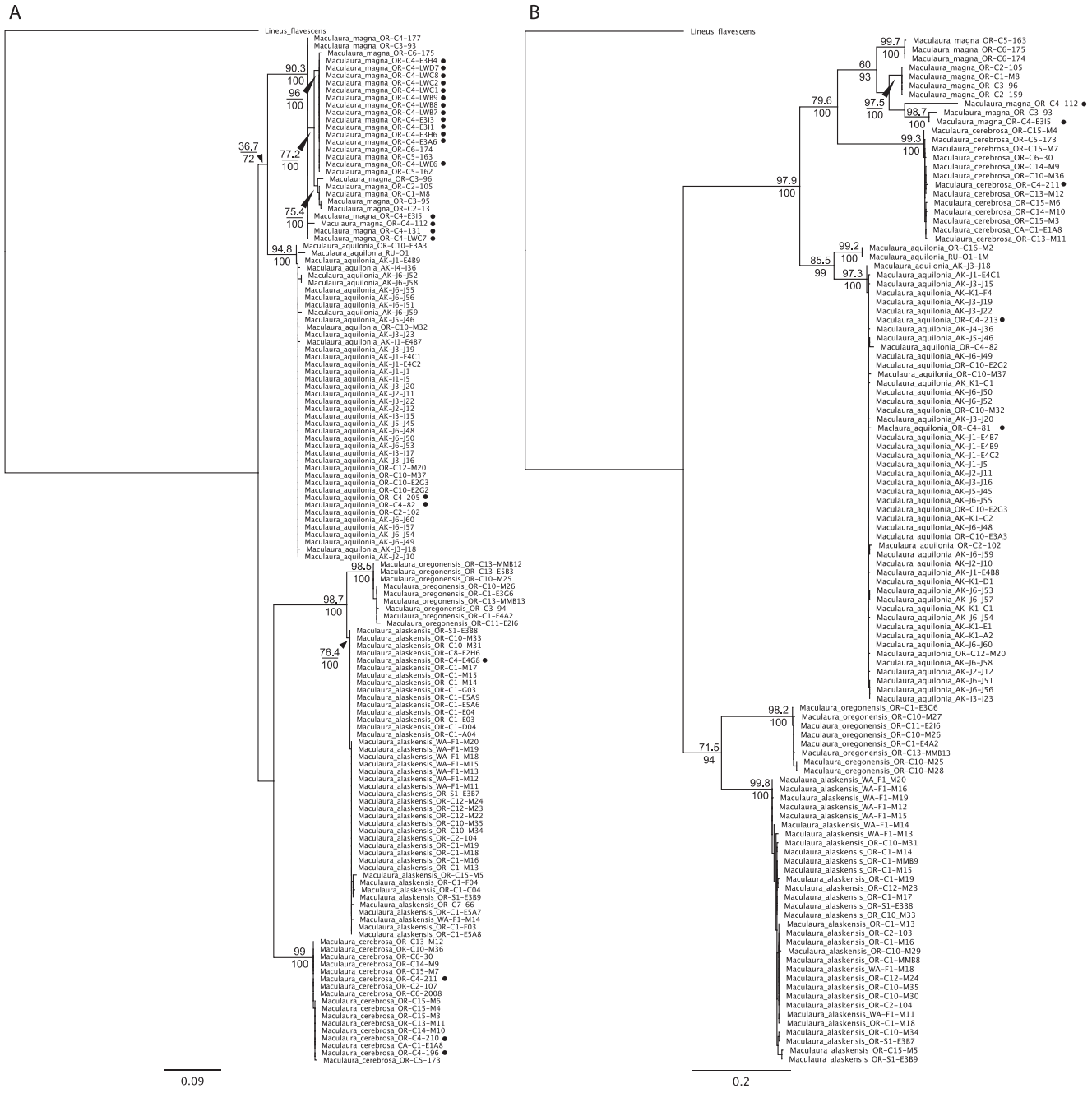

Fig. 12. **(A)** 16S and **(B)** COI maximum likelihood phylogenies for the genus *Maculaura* gen. nov. Bootstrap support value (> 70%) in maximum likelihood analysis (above node) and Bayesian posterior probabilities (below node) are indicated for each clade. Individual collection locations are shown and correspond to those in Fig. 1. Larval sequences are indicated with closed circles.

and *M. oregonensis*) (Fig. 13F–H), while *M. aquilonia* consists of two haplotype networks (Fig. 13I) and *M. magna*, exhibiting the greatest amount of genetic variation, comprises three haplotype networks (Fig. 13J) that cannot be connected using a 95% confidence interval. *Maculaura alaskensis* comprises 15 haplotypes (Fig. 13F); *M. cerebrosa*, eight haplotypes (Fig. 13G); and *M. oregonensis*, five haplotypes (Fig. 13H). *Maculaura aquilonia* is divided into two networks including 20 haplotypes; one network with one haplotype (from individuals found in both eastern and western Pacific) and the other with 19 (Fig. 13I). The three haplotype networks for *M. magna* include one network with a single haplotype, and two networks with two haplotypes each, one separated by one nucleotide and the other separated by seven nucleotide changes (Fig. 13J).

Nine species were revealed with the bPTP analysis using 16S and ten species using COI sequence data (Table 3). Analyses of 16S and COI sequences from *M. alaskensis*, *M. cerebrosa*, and *M. oregonensis* grouped them into one species each. *Maculaura magna* was partitioned into five groups in both analyses. *Maculaura aquilonia* was a single species according to 16S data, but was split into two spe-

Table 3. Comparison between different species delimitation methods. The five species described here are indicated in the top row; the number of taxa (i.e. species) suggested by each method are shown in the table. The total number of species in the genus *Maculaura* gen. nov. suggested by each method is shown at far right.

		Maculaura alaskensis	*Maculaura oregonensis*	*Maculaura aquilonia*	*Maculaura cerebosa*	*Maculaura magna*	total
morphology							
	adult	I	I	I	I	I	5
	gamete	I	I	I	I	I	5
16S							
	reciprocal monophyly	I	I	I	I	I	5
	statistical parsimony (TCS)	I	I	I	I	I	5
	ABGD	I		I	I	I	4
	bPTP	I	I	I	I	I I I I I	9
COI							
	reciprocal monophyly	I	I	I	I	I	5
	statistical parsimony (TCS)	I	I	I I	I	I I I	8
	ABGD	I	I	I I	I	I I I	9
	bPTP	I	I	I I	I	I I I I I	10

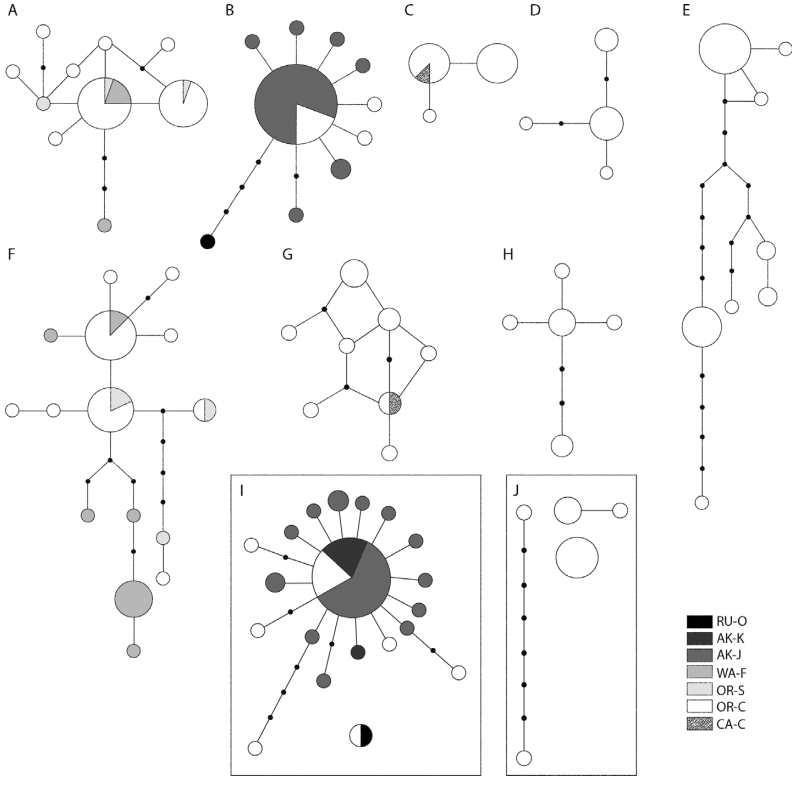

Fig. 13. **(A–E)** 16S rDNA and **(F–J)** COI haplotype networks for **(A, F)** *Maculaura alaskensis* comb. nov., **(B, I)** *Maculaura aquilonia* sp. nov., **(C, G)** *Maculaura cerebrosa* sp. nov., **(D, H)** *Maculaura oregonensis* sp. nov., **(E, J)** *Maculaura magna* sp. nov. Sample sites are shown for each haplotype. *Maculaura aquilonia* sp. nov. and *Maculaura magna* sp. nov. haplotypes did not group into a single network for the COI gene region and haplotypes associated with these species are surrounded by boxes (I, J).

cies in COI analysis.

Cross-fertilization experiments

Based on our observations, only three *Maculaura* species have somewhat overlapping reproductive timing: *M. alaskensis*, *M. aquilonia*, and *M. cerebrosa*. Reciprocal crosses were attempted between a single male and female each of *M. alaskensis* and *M. cerebrosa* on 8 July 2013 (one replicate each). Although sperm appeared to be attracted to the eggs, no cleavage occurred in either reciprocal cross. Control crosses, however, developed normally for both species. An additional cross (one replicate) was attempted between a single male *M. aquilonia* and female *M. cerebrosa* on 25 February 2014. This cross also resulted in no cleavage. Due to the lack of availability of both sexes during this time, control crosses were not attempted for *M. aquilonia* and *M. cerebrosa*; however, conspecific fertilization and larval culturing has been successful in the laboratory for each of these species at other times (see Figs. 8–10).

DISCUSSION

Integrative taxonomy of the "Micrura alaskensis" species complex

Although most species descriptions are limited to adult morphology, this information typically is not sufficient to differentiate between closely related or cryptic species (e.g. Manchenko and Kulikova, 1996; Hebert et al., 2004; Strand and Sundberg, 2005; Lavoué et al., 2010; Schulze et al., 2012). This, indeed, is the case for the "*Micrura alaskensis*" species complex. Often, cryptic species can be distinguished from each other by using additional kinds of data such as DNA sequences, gamete morphology, or other reproductive characters, an approach called integrative taxonomy (e.g. Chen et al., 2010; Puillandre et al., 2014; Welton et al., 2014). Here we present evidence from adult morphology, partial sequences of 16S and COI, gamete morphology, and interbreeding experiments to show that "*Micrura alaskensis*" is not one but five different species.

Some of these five species can be distinguished from each other based on external appearance of live adults

using characters such as shape, size, and color of body, and shape and size of the caudal cirrus. Other species are difficult to distinguish based on adult morphology alone. However, they can be easily differentiated using gamete morphology. While we lack information on the egg size of *Maculaura oregonensis,* the other four species can be differentiated by characteristics of the eggs (size and presence of chorion), with further support from sperm morphology. Interestingly, the presence of the chorion in the eggs of *M. cerebrosa* and *M. magna* correlates with modified sperm morphology (scimitar or spear-shaped sperm head). It is possible that a modified sperm head assists in penetrating the egg chorion in these species. Because changes in gamete morphology or other reproductive characteristics can form a barrier to fertilization, such changes are among the first differences one would expect to observe in recently diverged species (e.g. Landry et al., 2003). Indeed, our preliminary crossbreeding experiments (*M. alaskensis* × *M. cerebrosa*; *M. cerebrosa* × *M. aquilonia*) provide evidence that at least some of these species are reproductively isolated.

DNA taxonomy methods based on reciprocal monophyly, existence of separate haplotype networks in statistical parsimony analyses, and the presence of a barcoding gap are commonly used as evidence in support of separate species hypotheses (Hebert et al., 2003; Meyer and Paulay, 2005; Mahon et al., 2009; Chen et al., 2010; Bucklin et al., 2011). Here we show that the existence of five distinct lineages, corresponding to the five species described by us, is supported by reciprocal monophyly on both 16S and COI phylogenies (Fig. 12). Furthermore, statistical parsimony analysis of 16S sequence data supports the existence of the same five species (Fig. 13). Haplotype network analysis of COI sequence data results in one network for each of the three species, *M. alaskensis*, *M. cerebrosa*, and *M. oregonensis*. *Maculaura aquilonia* and *M. magna* are further split into two and four networks, respectively. This is not surprising because statistical parsimony analyses tends to over-split species compared to other methods of species delimitation (e.g. Jörer et al., 2012). The three species (*M. alaskensis*, *M. cerebrosa*, and *M. oregonensis*) were also supported by the bPTP and ABGD analyses of both data sets. These latter methods tended to over-split the species *M. magna* (both gene regions) and *M. aquilonia* (COI only) (Table 3). The same five species are also supported by the presence of a clear barcoding gap (Meyer and Paulay, 2005; Bucklin et al., 2011) between the maximum intraspecific uncorrected sequence divergences (1.1% for 16S and 7.1% for COI) and the minimum interspecific divergences (4.0% for 16S and 12.9% for COI). Species delimitation analyses suggest that *M. magna* and, to some extent *M. aquilonia*, may represent multiple species or are in the process of further speciation. In fact, we have noticed subtle differences in morphology (e.g. body color) among specimens of *M. magna*. However, we do not have sufficient information to confidently split species further than we have here. To sum it up, most of the molecular analyses support our designation of five species. If anything, we are being conservative, and it is possible that *M. magna* represents more than one species. Future sampling and studies of more individuals (their morphology, reproductive biology, and DNA sequence data) of this possibly diversifying species are needed to confirm or exclude this possibility.

Micrura griffini Coe, 1905

Coe (1905) described *Micrura griffini* based on specimens collected in San Pedro, California. This species resembled *Micrura alaskensis*, but was larger, more reddish in color and lacked accessory buccal glands (Coe, 1905). Despite these differences in morphology, Coe (1940) later synonymized these two species. We have not attempted to sample *Maculaura* specimens south of Crescent City, California and can only speculate on the identity of *Micrura griffini* as described by Coe (1905). The external morphology (e.g. size, body color), habitat, reproductive season and oocyte size are similar to *M. magna*. The accessory buccal glands are not as prominent in *M. magna* as they are in other *Maculaura* species (e.g. compare Figs. 5D, 7B, 7E with 7J), but are not lacking entirely, as Coe indicated for *Micrura griffini*. Several characters are distinctly different between the two species. First, the oocytes of *Micrura griffini* are described as being remarkably clear (Coe, 1905), which is not the case for *M. magna* (Fig. 3G). Second, Coe (1905) described a distinctly pink brain region for *Micrura griffini*. We have not observed this in *M. magna*, but only see it in *M. cerebrosa*. Furthermore, the body color of *Micrura griffini* was described as rosy, bright pinkish red or purplish. We have never observed purplish color in *M. magna* specimens. Thus it is possible that *Micrura griffini* represents a distinct species, possibly within *Maculaura* gen. nov. Future efforts must be directed toward obtaining samples from California for morphological and DNA analyses in order to assess the status of *Micrura griffini* Coe 1905.

Maculaura alaskensis versus *Maculaura aquilonia*

Although Coe (1901) originally described *Micrura alaskensis* from Alaska, his later revisions (Coe, 1904, 1905, 1943) expanded the range of this species south to Ensenada, Mexico, and his revised descriptions clearly include characteristics of more than one species. In fact, all the five species described here fit, at least in part, Coe's (1901, 1904, 1905, 1943) descriptions of "*Micrura alaskensis*". Because the type material does not exist, it is not clear which of the five species Coe (1901) originally encountered and described. DNA sequence data from *Micrura alaskensis*-like specimens, collected from two different locations in Alaska by ourselves and colleagues (albeit none of the locations mentioned in Coe's original description), matches the sequences of one of the five species described here (*M. aquilonia*), but, confusingly, not the one that all recent studies refer to as *Micrura alaskensis.* A literature search for "*Micrura alaskensis*" yields at least 29 publications by 26 authors (as of May 2015) ranging from 1987 to 2014 (Stricker, 1987, 2006; Stricker and Folsom, 1998; Stricker and Smythe, 2000, 2001, 2003; Stricker et al., 2001, 2013; Thollesson and Norenburg, 2003; Maslakova and Matz, 2005; Thiel and Junoy, 2006; Schwartz, 2009; Hiebert and Maslakova, 2010; McDonald and Grünbaum, 2010; Maslakova, 2010; Deguchi et al., 2011; Hiebert and Maslakova, 2012, 2014; Hiebert et al., 2013; Dassow and Maslakova, 2013; Dassow et al., 2013; Bartolomaeus et al.,

2014; Bird et al., 2014; Maslakova and Dassow, 2014; Mulligan et al., 2014; Swider et al., 2014; Maslakova and Hiebert, 2014; Hiebert and Maslakova, 2015). The species used in nearly every study can be linked by collection location, DNA sequence data, or personal observation to the only species of this complex that is currently known to occur in False Bay, San Juan Island, WA (*Maculaura alaskensis*) and also occurs in southern Oregon. It is distinct from the only species of the genus that we have encountered in Alaska.

We could, of course, assume that the species we found in Alaska (*Maculaura aquilonia*) was the same species originally encountered by Coe (1901), and retain the epithet "*alaskensis*" for it. This would be nomenclaturally straightforward. However, we believe that this would create a significant problem for a community of researchers who know "*Micrura alaskensis*" as a different species, and use it for cell biology, developmental biology, and other types of biological research. Importantly, some of these researchers are not systematists, and might find the name change confusing. It would be especially confusing because the name "*alaskensis*" would not be simply synonymized with another, but would apply to a different, closely related, and morphologically similar species.

In order to maintain nomenclatural stability and facilitate future research using these species, we chose to retain the specific epithet "*alaskensis*" for the species from Washington and Oregon used in recent studies cited above (and designated a neotype and a topogenetype from one of these locations), even though it is possible that it is not the species originally described by Coe (1901) from Alaska. It is possible that this species does occur in Alaska, but we have not encountered it. Moreover, even if it does not currently occur in Alaska, it is not inconceivable that it may expand its range northward in the future (e.g. Jones et al., 2012; Chust et al., 2014). To sum up, *Maculaura alaskensis* may not occur in Alaska, but it is the species that most researchers know as "*Micrura alaskensis*". On the other hand, *M. aquilonia* is the only member of the genus we have encountered in Alaska so far.

Support for the genus *Maculaura*

As members of the genus *Maculaura* all partially fit previous descriptions of *Micrura alaskensis* (Coe, 1901, 1904, 1905, 1940, 1943), characters previously considered exclusive to this species may represent synapomorphies for the new genus described here. For example, Coe (1901, 1940) noted peculiar species-specific "accessory buccal glands" (Coe, 1901, plate 13, fig. 1) in "*Micrura alaskensis*". These foregut glands are sub-epithelial, associated with the buccal cavity and their bodies often penetrate into the inner longitudinal musculature or extend beyond the circular musculature and into the ventral outer longitudinal musculature. Such glands occur in all *Maculaura* species, to varying degrees (Figs. 5, 7). Importantly, these glands are not observed in *Micrura fasciolata* (USNM# 1098168, Hiebert, Maslakova and Norenburg, personal observation), the type species of the genus *Micrura*. Furthermore, none of the nine species that are described (e.g. Riser, 1998) or coded in character matrices (Schwartz, 2009) as having similar glandular morphology to *Maculaura* (*Micrura wilsoni* USNM# 1107414, *Cerebratulus marginatus* USNM#s 1098145–46, *Zygeupolia rubens* USNM# 1098190, *Lineus viridis* USNM# 1098162, *Lineus rubescens* USNM# 1098157, *Fragilonemertes rosea* USNM# 170035, *Eousia verticivarius* USNM#s 1098166–67, *Micrura formosana* USNM# 1098170–71, *Notospermus geniculatus* USNM# 1098180) exhibit the accessory buccal gland cells observed in *Maculaura* spp. (Norenburg, personal communication). These glands were also not observed in two local undescribed lineiform species (*Micrura* sp. "dark" and *Micrura* sp. "not coei", Hiebert, personal observation).

Another morphological synapomorphy of the genus *Maculaura* may be the *pilidium maculosum* larval form characterized by the pigment spots on the juvenile amnion (Figs. 6, 10, 11). Larval development is known in four of the five species (Maslakova, 2010; this study). Three of those exhibit typical pigmentation pattern described here, and one species exhibits less prominent pigmentation (*Maculaura aquilonia*; Figs. 8, 9). To our knowledge this type of pigmentation has not been observed in any other species of pilidiophoran nemertean, whose larva is known. The development in the type species for the genus *Micrura* – *Micrura fasciolata*, is currently unknown. Lacalli (2005) described larvae of *pilidium maculosum* type from Bamfield Inlet, BC, Canada. Based on the fact that Bamfield is within the geographical range of *Maculaura*, it is very likely that those larvae belong to one of the species described here.

Aside from these morphological characters, the monophyly of *Maculaura* is supported by phylogenetic analyses of COI, 16S rDNA, and 28S rDNA sequence data, and the clade is only distantly related to *Micrura fasciolata* (Hiebert and Maslakova, in prep).

ACKNOWLEDGMENTS

We acknowledge support from the staff and faculty at the OIMB. We thank Sherry Tamone at the University of Alaska, Southeast for lab space while collecting specimens in Juneau, AK. George von Dassow, Laurel Hiebert and George Ayres helped collect many of the specimens used here. We thank Leif Rasmuson for aiding in preparation of Figure 1, and Patrick Beckers for the English translation of the diagnosis of *Micrura* from Otto Bürger's 1895 monograph. We thank Alexei V. Chernyshev, Hiroshi Kajihara, and Jon L. Norenburg for their opinions on the nomenclatural implications of our findings. We thank Alexei V. Chernyshev for providing specimens from Russia and examining three individuals with confocal microscopy. We also thank Gustav Paulay and Jon L. Norenburg for providing samples and sequence data from California and Alaska, respectively. We further thank Jon L. Norenburg for examining histological sections from 10 heteronemertean species and providing images of sectioned nemerteans stored at the USNM (e.g. *Micrura fasciolata*) as well as helpful comments on this manuscript. Finally, we thank three anonymous reviewers for thorough comments and edits, which improved this manuscript. This study was partially supported by the NSF grants 1120537 to SAM and 1030453 to Craig Young and SAM.

REFERENCES

Andrade SCS, Strand M, Schwartz M, Chen H, Kajihara H, Döhren Jv, et al. (2012) Disentangling ribbon worm relationships: multilocus analysis supports traditional classification of the phylum Nemertea. Cladistics 28: 141–159

Bartolomaeus T, Maslakova SA, Döhren Jv (2014) Protonephridia in the larvae of the palaeonemertean species *Carinoma mutabilis*

(Carinomidae, Nemertea) and *Cephalothrix* (*Procephalothrix*) *filiformis* (Cephalothricidae, Nemertea). Zoomorphology 133: 43–57

Bird AM, Dassow Gv, Maslakova SA (2014) How the pilidium larva grows. EvoDevo 5:13 doi: 10.1186/2041-9139-5-13

Bucklin A, Steinke D, Blanco-Bercial L (2011) DNA barcoding of marine Metazoa. Ann Rev Mar Sci 3: 471–508

Bürger O (1895) Die Nemertinen des Golfes von Neapel und der angrenzenden Meeres-Abschnitte. Fauna Flora Golf Neapel 22: 1–743

Chen H-X, Strand M, Norenburg JL, Sun S-C, Kajihara H, Chernyshev AV, et al. (2010) Statistical parsimony networks and species assemblages in cephalotrichid nemerteans (Nemertea). PLoS ONE 5(9): e12885 doi:10.1371/journal.pone.0012885

Chernyshev AV (2015) CLSM analysis of the phalloidin-stained muscle system of the nemertean proboscis and rhynchocoel. Zool Sci 32: 547–560

Chust G, Castellani C, Licandro P, Ibaibarriaga L, Sagarminaga Y, Irigoien X (2014) Are *Calanus* spp. shifting poleward in the North Atlantic? A habitat modeling approach. ICES J Mar Sci 71: 241–253

Clement M, Posada D, Crandall KA (2000) TCS: a computer program to estimate gene genealogies. Mol Ecol 9: 1657–1659

Coe WR (1901) Papers from the Harriman Alaska Expedition. XX. The nemerteans. Proc Wash Acad Sci 3: 1–110

Coe WR (1904) The nemerteans. Harriman Alaska Exped 11: 1–220

Coe WR (1905) Nemerteans of the west and northwest coasts of America. Bull Mus Comp Zool Harvard Coll 47: 1–318

Coe WR (1940) Revision of the nemertean fauna of the Pacific coasts of North, Central and northern South America. Allan Hancock Pac Exped 2: 247–323

Coe WR (1943) Biology of nemerteans of the Atlantic coast of North America. Trans Conn Acad Arts Sci 35: 129–328

Corrêa DD (1964) Nemerteans of California and Oregon. Proc Cal Acad Sci 31: 515–558

Dassow Gv, Maslakova SA (2013) How the pilidium larva pees. Integrat Comp Biol 53: E386

Dassow Gv, Emlet RB, Maslakova SA (2013) How the pilidium larva feeds. Front Zool 10: 47

Deguchi R, Takeda N, Stricker SA (2011) Comparative biology of cAMP-induced germinal vesicle breakdown in marine invertebrate oocytes. Mol Reprod Devel 78: 708–725

Ehrenberg CG (1828, 1831) Phytozoa turbellaria Africana et Asiatica in Phytozoorum Tabula IV et V delineata. In "Symbolae physicae, seu icones et descriptiones corporum naturalium novorum aut minus cognitorum quae ex itineribus per Libyam, Aegyptium, Nubiam, Dongalam, Syriam, Arabiam et Habessiniam, pars zoologica II, anima" Ed by FG Hemprich, CG Ehrenberg, Officina Academica, Berlin, pp 53–67, pls IV–V (plates published in 1828, text in 1831)

Felsenstein J (1985) Confidence limits on phylogenies: an approach using the bootstrap. Evolution 39: 783–791

Folmer O, Black M, Hoeh W, Lutz R, Vrijenhoek R (1994) DNA primers for amplification of mitochondrial cytochrome c oxidase subunit I from diverse metazoan invertebrates. Mol Mar Biol Biotech 3: 294–299

Gibson R (1995) Nemertean genera and species of the world: an annotated checklist of original names and description citations, synonyms, current taxonomic status, habitats and recorded zoogeographic distribution. J Nat Hist 29: 271–562

Guindon S, Dufayard J-F, Lefort V, Anisimova M, Hordijk W, Gascuel O (2010) New algorithms and methods to estimate maximum-likelihood phylogenies: assessing the performance of PhyML 3.0. Syst Biol 59: 307–321

Hart MW, Sunday J (2007) Things fall apart: biological species form unconnected parsimony networks. Biol Lett 3: 509–512 doi: 10.1098/rsbl.2007.0307

Hebert DN, Cywinska A, Ball SL, deWaard JR (2003) Biological identifications through DNA barcodes. Proc R Soc Lond B 270: 313–321

Hebert DN, Penton EH, Burns JM, Janzen DH, Hallwachs W (2004) Ten species in one: DNA barcoding reveals cryptic species in the neotropical skipper butterfly *Astraptes fulgerator.* PNAS 101: 14812–14817

Hiebert LS, Maslakova SA (2010) Axes and organs in nemertean larvae: development of a hoplonemertean. Int Comp Biol 50: E74

Hiebert LS, Maslakova SA (2012) Comparing axial patterning in nemertean larvae—insights into the evolution of a novel larval body plan. Int Comp Biol 52: E263

Hiebert LS, Maslakova SA (2014) How the pilidium larva uses Hox genes. Int Comp Biol 54: E90

Hiebert LS, Maslakova SA (2015) Hox genes pattern the anterior-posterior axis of the juvenile but not the larva in a maximally-indirect developing invertebrate, *Micrura alaskensis* (Nemertea). BMC Biol 13: 23 doi: 10.1186/s12915-015-0133-5

Hiebert TC, von Dassow G, Hiebert LS, Maslakova SA (2013) The peculiar nemertean larva *pilidium recurvatum* belongs to *Riserius* sp., a basal heteronemertean that eats *Carcinonemertes errans*, a hoplonemertean parasite of Dungeness crab. Invert Biol 132: 207–225 doi: 10.1111/ivb.12023

International Commission on Zoological Nomenclature (1999) International Code of Zoological Nomenclature, 4th ed. International Trust for Zoological Nomenclature, London

Iwata F (1954) The fauna of Akkeshi Bay XX. Nemertini in Hokkaido. J Fac Sci Hokkaido Univ Ser VI Zool 12: 1–39

Jones SJ, Southward AJ, Wethey DS (2012) Climate change and historical biogeography of the barnacle *Semibalanus balanoides*. Global Ecol Biogeogr 21: 716–724

Jörger KM, Norenburg JL, Wilson NG, Schroedl M (2012) Barcoding against a paradox? Combined molecular species delineations reveal multiple cryptic lineages in elusive meiofaunal sea slugs. BMC Evol Biol 12: 245

Kajihara H (2007) A taxonomic catalogue of Japanese nemerteans (phylum Nemertea). Zool Sci 24: 287–326

Kvist S, Laumer CE, Junoy J, Giribet G (2014) New insights into the phylogeny, systematics and DNA barcoding of Nemertea. Invertebr Syst 28: 287–308

Lacalli T (2005) Diversity of form and behaviour among nemertean pilidium larvae. Acta Zool 88: 267–276

Lavoué S, Miya M, Arnegard ME, McIntyre PB, Mamonekene V, Nishida M (2010) Remarkable morphological stasis in an extant vertebrate despite tens of millions of years of divergene. Proc R Soc B 278: 1003–1008 doi: 10.1098/rspb.2010.1639

Landry C, Geyer LB, Arakaki Y, Uehara T, Palumbi SR (2003) Recent speciation in the Indo-West Pacific: rapid evolution of gamete recognition and sperm morphology in cryptic species of sea urchin. Proc Biol Sci 270: 1839–1847

Leasi F, Norenburg J (2014) The necessity of DNA taxonomy to reveal cryptic diversity and spatial distribution of meiofauna, with a focus on Nemertea. PLoS ONE 9(8): e104385 doi: 10.1371/journal.pone.0104385

Mahon AR, Thornhill DJ, Norenburg JL, Halanych KM (2009) DNA uncovers Antarctic nemertean biodiversity and exposes a decades-old cold case of asymmetric inventory. Polar Biol 33: 193–202

Manchenko GP, Kulikova VI (1996) Enzyme and colour variation in the hoplonemertean *Tetrastemma nigrifrons* from the Sea of Japan. Hydrobiologia 337: 69–76

Maslakova SA (2010) Development to metamorphosis of the nemertean pilidium larva. Front Zool 7: 30 doi: 10.1186/1742-9994-7-30

Maslakova SA, Dassow Gv (2014) How the pilidium larva escapes

an ancient constraint. Int Comp Biol 54: E134
Maslakova SA, Hiebert TC (2014) From trochophore to pilidium and back again—a larva's journey. Int J Devel Biol 58: 585–591 doi: 10.1387/ijdb.140090sm
Maslakova SA, Matz MV (2005) Evolution of larval development in nemerteans (phylum Nemertea). Int Comp Biol 45: 1164
McDonald KA, Grünbaum D (2010) Swimming performance in early development and the "other" consequences of egg size for ciliated planktonic larvae. Int Comp Biol 50: 589–605
McIntosh WC (1873–1874) A Monograph of the British Annelids Part I: The Nemerteans. Ray Society, London
Meyer CP, Paulay G (2005) DNA barcoding: error rates based on comprehensive sampling. PLoS Biol 3(12): e422
Mulligan KL, Hiebert TC, Jeffery NW, Gregory TR (2014) First estimates of genome size in ribbon worms (phylum Nemertea) using flow cytometry and Fleugen image analysis densitometry. Can J Zool 92: 847–851
Niesen TM (2007) Intertidal habitats and marine biogeography of the Oregonian Province. In "The Light and Smith Manual: Intertidal Invertebrates from Central California to Oregon, 4th ed" Ed by JT Carlton, University of California Press, Berkeley, pp 3–17
Palumbi S, Martin A, Romano S, McMillan WO, Stice L, Grabowski G (1991) The simple fools guide to PCR Version 2.0. Department of Zoology Kewalo Marine Laboratory, University of Hawaii, Honolulu
Posada D (2008) jModelTest: phylogenetic model averaging. Mol Biol Evol 25: 1253–1256
Puillandre N, Lambert A, Brouillet S, Achaz G (2012) ABGD, automatic barcode gap discovery for primary species delimitation. Mol Ecol 21: 1864–1877
Puillandre N, Stöcklin R, Favreau P, Bianchi E, Perret F, Rivasseau A, et al. (2014) When everything converges: integrative taxonomy with shell, DNA and venomic data reveals *Conus conco*, a new species of cone snails (Gastropoda: Conoidea). Mol Phylogenet Evol 80: 186–192
Rambaut A (2009) FigTree version 1.3.1 [http://tree.bio.ed.ac.uk/software/figtree/]
Roe P, Norenburg JL, Maslakova SA (2007) Nemertea. In "The Light and Smith Manual: Intertidal Invertebrates from Central California to Oregon 4th Edition" Ed by JT Carlton, University of California Press, Berkeley, pp 221–230
Riser NW (1998) The morphology of *Micrura leidyi* (Verrill, 1892) with consequent systematic revaluation. Hydrobiologia 365: 149–156
Ronquist F, Teslenko M, Van Der Mark P, Ayres DL, Darling A, Höhna S, et al. (2012) MrBayes 3.2: efficient Bayesian phylogenetic inference and model choice across a large model space. Syst Biol 61: 2010–2013
Schulze A, Maiorova A, Timm LE, Rice ME (2012) Sipunculan larvae and "cosmopolitan" species. Int Comp Biol 52: 497–510
Schwartz ML (2009) Untying a Gordian Knot of Worms: Systematics and Taxonomy of the Pilidiophora (phylum Nemertea) from Multiple Data Sets. Ph.D. thesis, Columbian College of Arts and Sciences, George Washington University, Washington, DC
Strand M, Sundberg P (2005) Delimiting species in the hoplonemertean genus *Tetrastemma* (phylum Nemertea): morphology is not concordant with phylogeny as evidence from mtDNA sequences. Biol J Linn Soc 86: 201–212
Stricker SA (1987) Nemertea. In "Reproduction and Development of Marine Invertebrates of the Northern Pacific Coast" Ed by M Strathmann, University of Washington Press, Seattle, pp 94–101
Stricker SA (2006) Structural reorganizations of the endoplasmic reticulum during egg maturation and fertilization. Semin Cell Dev Biol 17: 303–313
Stricker SA, Cline C, Goodrich D (2013) Oocyte maturation and fertilization in marine nemertean worms: using similar sorts of signaling pathways as in mammals, but often with differing results. Biol Bull 224: 137–155
Stricker SA, Folsom MW (1998) A comparative ultrastructural analysis of spermatogenesis in nemertean worms. Hydrobiologia 365: 55–72
Stricker SA, Smythe TL (2000) Multiple triggers of oocyte maturation in nemertean worms: The roles of calcium and serotonin. J Exp Zool 287: 243–261
Stricker SA, Smythe TL (2001) 5-HT causes an increase in cAMP that stimulates, rather than inhibits, oocyte maturation in marine nemertean worms. Development 128: 1415–1427
Stricker SA, Smythe TL (2003) Endoplasmic reticulum reorganizations and Ca^{2+} signaling in maturing and fertilized oocytes of marine protostome worms: the roles of MAPKs and MPF. Development 130: 1867–2879
Stricker SA, Smythe TL, Miller L, Norenburg JL (2001) Comparative biology of oogenesis in nemertean worms. Acta Zool 82: 213–230
Sundberg P, Saur M (1998) Molecular phylogeny of some European heteronemertean (Nemertea) species and the monophyletic status of *Riseriellus*, *Lineus* and *Micrura*. Mol Phylogenet Evol 10: 271–280
Swider A, Hiebert LH, Dassow Gv, Maslakova SA (2014) Expression and function of *Otx* during ciliated band development in the pilidium larva. Integrat Comp Biol 54: E356
Tamura K, Nei M (1993) Estimation of the number of nucleotide substitutions in the control region of mitochondrial DNA in humans and chimpanzees. Mol Biol Evol 10(3): 512–526
Thiel M, Junoy J (2006) Mating behavior of nemerteans: present knowledge and future directions. J Nat Hist 40: 1021–1034
Thollesson M, Norenburg JL (2003) Ribbon worm relationships—a phylogeny of the phylum Nemertea. Proc R Soc Lond B 270: 407–415
Welton LJ, Travers SL, Siler CD, Brown RM (2014) Integrative taxonomy and phylogeny-based species delimitation of Philippine water monitor lizards (*Varanus salvator* complex) with descriptions of two new cryptic species. Zootaxa 3881: 201–227
Yamaoka T (1940) The fauna of Akkeshi Bay. IX. Nemertini. J Fac Sci Hokkaido Univ Ser 6 Zool 7: 205–261
Zhang J, Kapli P, Pavlidis P, Stamatakis A (2013) A general species delimitation method with applications to phylogenetic placements. Bioinformatics 29(22): 2869–2876

(Received January 22, 2015 / Accepted May 27, 2015)